photochem

MDPI

Review

Stability and Degradation in Dye-Sensitized Solar Cells: An Interface-Centred and Evidence-Based Review

Liviu Olteanu [1] and Sofia Slămnoiu-Teodorescu [2,*]

[1] Institute of Multidisciplinary Research for Science and Technology, Valahia University of Targoviste, 13 Sinaia Alley, 130004 Targoviste, Romania; liviu.olteanu@valahia.ro
[2] Faculty of Materials Engineering and Mechanics, Valahia University of Targoviste, 13 Sinaia Alley, 130004 Targoviste, Romania
* Correspondence: sofia.teodorescu@valahia.ro

Abstract

Dye-sensitized solar cells (DSSCs) have attracted sustained research interest due to their low-cost fabrication, tunable optoelectronic properties, and compatibility with diverse substrates. Despite substantial advances in power conversion efficiency, long-term operational stability remains the principal barrier to large-scale deployment. Device degradation arises from complex and coupled processes involving sensitizer instability, interfacial recombination, electrolyte volatility, and electrode corrosion, all strongly governed by surface chemistry and interfacial structure. This review provides a comprehensive analysis of stability and degradation mechanisms in DSSCs, integrating molecular-level transformations with interface-driven phenomena and materials-related limitations. Particular attention is given to dye photodegradation and desorption, TiO_2 surface states, transparent conductive oxide instability, and electrolyte-induced corrosion. Surface engineering strategies—including passivation layers, protective coatings, and encapsulation approaches—are critically evaluated in relation to their effectiveness under different ageing conditions. Particular emphasis is placed on distinguishing directly supported degradation mechanisms from interpretations based primarily on device-level performance decay. By linking operational stressors, molecular and interfacial changes, diagnostic signatures, and mitigation strategies, this review provides an interface-centred framework for assessing DSSC stability and identifying rational pathways towards more durable device architectures. To make this distinction explicit, the literature is organised into three evidence levels: (i) ageing studies supported by independent chemical, structural, spectroscopic, microscopic, or electrochemical diagnostics, (ii) device-level retention studies without direct mechanistic confirmation, and (iii) performance/design studies with potential stability implications but without dedicated ageing evidence. Stability-testing approaches are also interpreted according to their specific stress conditions rather than treated as a common lifetime scale.

Keywords: dye-sensitized solar cells; stability; degradation; dye/TiO_2 interface; electrolyte; surface passivation; encapsulation; ageing

Check for updates

Academic Editor: Marcelo Guzman

Received: 25 September 2026
Revised: 4 November 2026
Accepted: 11 November 2026
Published: 16 November 2026

Copyright: © 2026 by the authors. Licensee MDPI, Basel, Switzerland. This article is an open access article distributed under the terms and conditions of the Creative Commons Attribution (CC BY) license.

1. Introduction

1.1. Technological Background and Relevance of DSSCs

Dye-sensitized solar cells (DSSCs) are a distinctive third-generation photovoltaic technology in which light absorption, charge separation, and charge transport are distributed across molecular and nanostructured components rather than confined to a conventional solid-state p–n junction.

The mesoscopic TiO_2 architecture introduced by O'Regan and Grätzel established a practical route to low-temperature photovoltaic fabrication, while the broader photoelectrochemical framework demonstrated the value of separating photon capture from charge transport [1,2]. This modular architecture remains technologically important because the sensitizer, semiconductor oxide, redox mediator, catalytic counter electrode, and transparent conductive substrate can be optimised independently, enabling the development of lightweight, semi-transparent devices with tunable optical properties [3,4]. Subsequent advances in molecular engineering demonstrated that DSSCs are not intrinsically limited to modest efficiencies. Porphyrin sensitizers combined with cobalt redox shuttles exceeded 12% power conversion efficiency, subsequent molecular optimisation yielded devices with efficiencies of approximately 13%, and co-sensitisation strategies further improved performance [5–7]. A second technological niche has emerged under diffuse and artificial illumination, where spectral matching and high photovoltage can be more important than the high current densities targeted under full-sun conditions.

Co-sensitised, copper-mediated cells have therefore become important reference systems for indoor energy harvesting and autonomous sensor nodes [8]. These characteristics make durability, rather than efficiency alone, a decisive parameter for translating laboratory-scale devices into deployable products. Recent research illustrates the diversification of DSSC architectures, encompassing advanced sensitizer design [9], indoor and low-light operation [10,11], sensitizer–performance relationships [12], transparent and bifacial devices [13,14], tandem configurations [15,16], natural-dye systems [17,18], and stability-oriented bifacial designs [19]. This diversification also implies that stability requirements are application-dependent, because indoor, transparent, bifacial, and tandem devices operate under different optical, thermal, electrical, and encapsulation constraints.

Application-dependent relevance is particularly important when DSSCs are compared with newer photovoltaic technologies. Although crystalline-silicon and perovskite devices achieve higher one-sun conversion efficiencies, DSSCs retain application-specific advantages under diffuse and artificial illumination, in semi-transparent and bifacial configurations, and in spectrally selective systems for building-integrated and agrivoltaic applications [13–21]. For these application areas, optical transmittance, colour tunability, spectral matching, low-light voltage, and long-duration autonomous operation may be more relevant than peak AM1.5G efficiency. Current solar-energy research also highlights the importance of spectral and interfacial engineering, ranging from ultrabroadband absorbers based on titanium nitride (TiN) to transport-layer optimisation in lead-free perovskite devices [22,23]; in DSSCs, analogous optical and interfacial control must be considered together with chemical durability.

1.2. The Efficiency–Durability Trade-Off

The same design choices that improve initial power conversion efficiency can introduce new ageing pathways. High-surface-area TiO_2 increases sensitizer loading but also enlarges the interfacial area available for surface reactions and recombination. More strongly oxidising redox couples can increase open-circuit voltage, but they also impose more stringent requirements on chemical compatibility with sensitizers, additives, catalysts, and sealing materials.

Highly conjugated sensitizers broaden light absorption but can be vulnerable to photooxidation, aggregation, or degradation of anchoring groups unless appropriate molecular protection is incorporated. Recent analyses of electrolytes and sensitizers therefore frame DSSC optimisation as a multi-objective problem in which charge transport, energetics, and chemical stability must be balanced simultaneously [24–26].

A stability-centred interpretation also changes how performance records are evaluated. A small reduction in initial power conversion efficiency (PCE) can be acceptable if the architecture suppresses solvent loss, stabilises the sensitizer/TiO_2 junction, or limits interfacial recombination over substantially longer operating periods. Conversely, a high initial PCE is of limited practical value when it depends on volatile solvents, poorly protected interfaces, or components that undergo chemical changes during prolonged illumination and thermal exposure.

This review therefore treats efficiency and durability as coupled design variables rather than independent optimisation targets. Recent experimental and computational studies likewise show that improvements in light absorption, charge transport, and sensitizer architecture should be evaluated together with recombination losses and stability constraints [12,27–33].

Consequently, reported stability improvements should not be interpreted from PCE retention alone, but in relation to the applied ageing conditions, device architecture, and diagnostic evidence used to identify the underlying degradation process.

Accordingly, the one-sun efficiency gap should not be interpreted as a universal measure of technological relevance. Recent perovskite-stability literature likewise shows that high efficiency and long-term operational durability remain distinct optimisation targets in emerging photovoltaics [34,35]. For DSSCs, the appropriate benchmark is therefore application-specific, particularly for indoor, semi-transparent, bifacial, and low-light operation.

1.3. Stability as the Primary Limitation to Commercialisation

Commercial reliability requires resistance to thermal cycling, continuous illumination, ultraviolet radiation, oxygen and water ingress, electrical bias conditions, and repeated redox turnover. Classical accelerated-ageing studies have shown that DSSCs can degrade at elevated temperatures even when macroscopic electrolyte leakage is prevented, demonstrating that intrinsic chemical instability cannot be addressed by packaging alone [36].

The electrical operating state is also important: cells held at short circuit can age differently from cells operated near the maximum power point or under open-circuit conditions. Laboratory protocols that do not define the electrical operating state may therefore misrepresent degradation rates under practical operating conditions [37]. At the component level, degradation mechanisms are strongly coupled. Electrolyte cations can modify TiO_2 trap-state populations during ageing; degradation at the sensitized TiO_2/electrolyte interface can alter recombination and charge transport; and ageing-induced increases in resistance can affect the short-circuit current density (J_{SC}), open-circuit voltage (V_{OC}), and fill factor (FF) in different ways [38,39].

Conductive substrates introduce an additional materials constraint because fluorine-doped tin oxide (FTO), indium tin oxide (ITO), and other transparent conducting oxides (TCOs) differ markedly in thermal and chemical robustness [40]. The central challenge to commercialisation is therefore not the instability of a single component, but the behaviour of an interacting system in which molecular, interfacial, and module-level ageing processes can reinforce one another.

This mechanistic coupling also limits the evidential value of photovoltaic performance decay alone: changes in J_{SC}, V_{OC}, or FF can indicate several competing degradation pathways and should therefore be regarded as diagnostic signatures rather than direct proof of a specific mechanism unless supported by complementary chemical, structural, or electrochemical measurements.

1.4. Scope and Organisation of This Review

This review develops an interface-centred framework for understanding DSSC stability. Operational stressors are first considered in terms of photoinduced, thermal, environmental, and electrical contributions. The discussion then follows the degradation sequence from sensitizer chemistry to the sensitizer/TiO_2 interface, conductive layers, and electrolyte.

Surface passivation, hydrophobic modification, protective layers, and encapsulation are evaluated according to the degradation pathways they are intended to mitigate. Finally, ageing protocols and photovoltaic performance signatures are linked to specific degradation mechanisms, while emerging solid-state, multilayer-barrier, and data-driven strategies are assessed. Particular emphasis is placed on mechanistic studies and primary experimental reports, with review articles used mainly to establish broader context. The distinctive perspective of the present work is an interface-centred and mechanism-oriented framework that links operational stressors to molecular and interfacial degradation processes, diagnostic signatures, and corresponding stability-engineering strategies. Particular attention is given to distinguishing degradation mechanisms supported by direct chemical, structural, or electrochemical evidence from those inferred mainly from device-level performance changes.

The literature selection prioritised recent peer-reviewed studies addressing DSSC degradation mechanisms, ageing behaviour, stability-oriented materials, and interface-engineering strategies, with particular emphasis on primary experimental reports published in recent years. Earlier studies were retained where they established foundational device concepts, diagnostic approaches, or uniquely relevant long-term stability evidence.

Recent DSSC reviews have addressed stability from different perspectives. Earlier work distinguished assumptions from experimentally supported degradation processes [41], whereas more recent reviews have focused on liquid-electrolyte commercialisation [42], broad component optimisation and characterisation [43], high-performance materials and fabrication strategies [44,45], or sensitizer molecular engineering and photostability [26]. The present review complements these contributions by applying three cross-cutting questions throughout the device stack: which stressor was applied, what material or interfacial change was actually measured, and whether the proposed mitigation strategy suppresses a demonstrated degradation mechanism or primarily improves a device-level metric. This evidence-oriented synthesis constitutes the principal added value of the review.

1.5. Review Methodology and Evidence Classification

This article is a narrative review with a structured literature-selection strategy rather than a systematic review or meta-analysis. The literature base was developed through a targeted assessment of recent peer-reviewed specialist literature addressing DSSC stability, degradation mechanisms, ageing behaviour, stability-oriented materials, and interface-engineering strategies. Peer-reviewed English-language studies were prioritised when they reported DSSC ageing, long-term operation, degradation diagnostics, stability-oriented materials, or interface-engineering strategies.

Studies concerned only with initial efficiency were retained only when they provided a mechanistically relevant design implication and are explicitly treated as performance/design evidence rather than as demonstrated stability improvement.

Foundational older studies were retained when they established long-term tests, diagnostic approaches, or degradation mechanisms not superseded by later work. Non-DSSC photovoltaic studies were included only for clearly identified cross-technology methodological comparisons. Relevant studies were assessed in terms of device architecture, stress conditions, performance evolution, and available independent diagnostics. Because the objective is critical mechanistic synthesis rather than exhaustive effect-size estimation, no PRISMA-style systematic screening or meta-analysis was undertaken. To make the strength

of evidence explicit, the discussion uses three evidence classes. Class A denotes ageing studies in which a proposed degradation mechanism is supported by at least one independent chemical, structural, spectroscopic, microscopic, or electrochemical diagnostic in addition to photovoltaic measurements. Class B denotes device-level retention or ageing studies in which stability is demonstrated by time-dependent electrical performance but the dominant mechanism is not independently confirmed. Class C denotes performance or design studies without a dedicated ageing experiment; these studies can motivate stability hypotheses or engineering choices but are not presented as proof of improved durability. This hierarchy is applied in the comparative tables and in the interpretation of representative studies.

2. Operational Stress Conditions Governing Device Stability

2.1. Photoinduced and UV-Related Stress

Illumination drives the intended photovoltaic cycle but can also promote parasitic photochemical reactions. TiO_2 absorbs in the ultraviolet region and can generate highly reactive charge carriers that interact with nearby organic species when interfacial scavenging is incomplete. Sensitizer oxidation, solvent reactions, redox imbalance, and degradation of polymeric sealing materials can therefore be accelerated by high-energy spectral components that contribute little to useful visible-light conversion. The importance of ultraviolet management was recognised in early stability studies and remains relevant to contemporary DSSC architectures [36].

The effect of illumination is strongly architecture-dependent. In thermal-stability studies of wavelength-selective DSSCs, a yellow sensitizer that also acted as a UV filter reduced ultraviolet exposure of internal device components, while the TiO_2 polymorph influenced anchoring stability and recombination behaviour [20]. This finding illustrates a broader design principle: spectral management can contribute to stability rather than serving solely as an optical optimisation strategy. UV-absorbing cover layers, sensitizers with tailored high-energy absorption, and chemically inert interlayers should therefore be evaluated together with the photocatalytic activity of the oxide and the redox chemistry of the electrolyte. Recent studies of transparent cells and natural sensitizers further support the role of spectral selectivity and sensitizer chemistry in determining both optical response and durability [13,17,33,46]. However, improved stability under reduced UV exposure should not be interpreted as evidence for a single degradation pathway unless supported by direct measurements of sensitizer integrity, interfacial chemistry, or electrolyte composition.

2.2. Thermal Stress and Temperature-Activated Processes

Elevated temperature accelerates diffusion, desorption, seal creep, and chemical reaction rates while increasing solvent vapour pressure. At the sensitizer/TiO_2 interface, heating can shift adsorption equilibria and promote sensitizer desorption or displacement by electrolyte species. In the electrolyte, higher temperature can initially enhance ionic transport while simultaneously accelerating solvent loss, ligand exchange, and parasitic reactions.

Because these effects can act in opposing directions, short-term thermal measurements may show improved current or fill factor even when the long-term chemical evolution is unfavourable. Recent work has quantified DSSC temperature coefficients and linked thermal response to TiO_2 polymorphism and sensitizer anchoring, showing that the temperature dependence of J_{SC}, V_{OC}, and maximum power can be strongly influenced by interfacial properties rather than by the bulk electrolyte alone [20].

Long-term stability requires more than tolerance to elevated temperatures; the device should preserve sensitizer anchoring, redox composition, and charge-transfer kinetics during repeated heating and cooling cycles. Temperature-dependent studies on indoor modules and hybrid photovoltaic systems further underline the need to evaluate thermal

response under the intended operating irradiance rather than under a single standard test condition [11,47,48].

Accordingly, thermal-stability results obtained at different temperatures, irradiances, and exposure durations should not be compared solely on the basis of PCE retention, because the balance between reversible transport effects and irreversible chemical degradation may differ substantially between test conditions.

2.3. Moisture and Oxygen Exposure

Water and oxygen can enter through seal edges, electrolyte-filling ports, polymeric barriers, and microscopic defects. Their effects extend beyond simple dilution of the electrolyte. Water can alter oxide-surface protonation, shift TiO_2 energetic levels, influence sensitizer binding, and redistribute ionic species; oxygen can participate in redox side reactions and promote oxidative degradation of organic components. In practical modules, ingress pathways are often localised, producing spatially heterogeneous ageing before a macroscopic decrease in PCE is detected.

Long-term outdoor studies show that hydrophobic surface chemistry can mitigate these effects. DSSC modules using long-chain alkyl-benzimidazole additives for hydrophobic passivation, together with strategies to limit iodine-species redistribution, retained approximately 75% of their initial performance after 12 years of outdoor exposure [49]. This long-term outdoor result is particularly valuable because it reflects combined environmental stresses, but it should not be directly compared with accelerated laboratory retention values obtained under controlled thermal or light-soaking conditions.

Hermetic glass-frit encapsulation provides a complementary approach by suppressing environmental ingress, thereby allowing intrinsic device chemistry to be assessed with reduced interference from leakage or moisture penetration [50,51]. Moisture stability is therefore best addressed through a combination of molecular-scale water rejection and low-permeability encapsulation.

2.4. Electrochemical and Electrical Bias Stress

DSSCs operate under sustained redox cycling, and the electrical boundary condition can influence chemical ageing. The oxidised sensitizer, reduced and oxidised mediator species, and charged surface states reach different steady-state populations under open-circuit, short-circuit, and maximum-power-point conditions.

Experimental ageing studies have shown that cells maintained at short circuit can degrade substantially faster than otherwise similar cells operated at open circuit or near the maximum power point [37]. This observation is important because many accelerated-ageing tests specify illumination and temperature but do not define the electrical operating state.

Electrochemical stress also involves repeated catalyst turnover, mediator diffusion, additive redistribution, and local potential gradients across porous electrodes.

Cobalt- and copper-based complexes can increase photovoltage but introduce ligand-sensitive chemistry, whereas the iodide/triiodide redox couple can be chemically aggressive towards some metallic and catalytic materials [25]. Reliable stability protocols should therefore report electrical loading conditions, mediator composition, and electrolyte volume together with conventional ageing variables.

Without this information, apparently conflicting stability results may reflect differences in electrochemical operating conditions rather than intrinsic differences in material stability.

Recent electrochemical studies of sensitizer regeneration, copper-redox/additive coordination, and alternative copper-mediated architectures further demonstrate how mediator speciation can influence recombination and long-term device response [52–58]. The relationship between the normal charge-transfer sequence and the principal molecular, interfa-

cial, electrolyte-related, and charge-collector-related degradation pathways is summarised schematically in Figure 1.

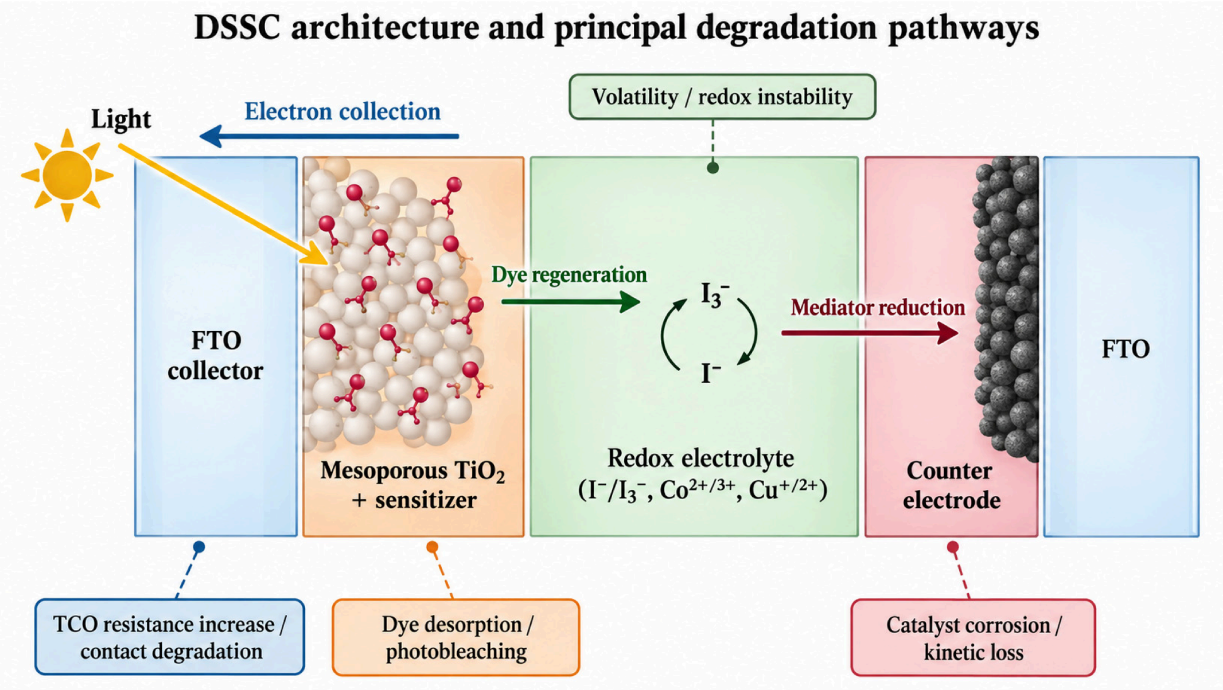


Figure 1. DSSC architecture and principal degradation pathways. The schematic distinguishes the functional charge-transfer sequence from the main molecular, interfacial, electrolyte-related, and charge-collector-related degradation processes.

The available evidence therefore supports electrical boundary conditions as an important contributor to ageing behaviour, but the resulting performance changes should be interpreted together with mediator-speciation and interfacial diagnostics before assigning a dominant chemical degradation mechanism.

Across these stressors, degradation should be considered across the complete current-generating and current-collecting stack. UV exposure primarily challenges the sensitizer, TiO_2 surface chemistry, electrolyte, and polymeric seals; elevated temperature additionally accelerates solvent loss, catalyst ageing, seal creep, and contact degradation; moisture and oxygen ingress can alter photoanode and redox chemistry while poisoning counter-electrode catalysts and promoting corrosion at exposed metallic collectors; and electrical bias can drive mediator redistribution, catalyst turnover, local potential gradients, and corrosion of module grids or interconnects.

In large-area parallel-grid modules, the latter issue is particularly important because silver, although highly conductive, is susceptible to corrosion in iodide/triiodide electrolytes, which can increase series resistance and contaminate the electrolyte [59,60]. Thus, the same external stress may generate different failure locations, and the affected component should be identified using component-specific diagnostics rather than inferred from a common decline in PCE.

Table 1 indicates that operational stressors can affect several device components simultaneously, making it difficult to identify the dominant degradation mechanism from a single electrical parameter. Reliable diagnosis therefore requires correlating the evolution of J_{SC}, V_{OC}, FF, and PCE with complementary spectroscopic, electrochemical, and package-level measurements.

Table 1. Operational stressors, primary degradation targets, and diagnostic signatures in DSSCs.

Stressor	Primary Vulnerable Components	Typical Device Signature	Recommended Diagnostics	References
UV/high-energy photons	Sensitizer; TiO_2 surface; electrolyte; polymeric seal	J_{SC} loss; V_{OC} drift; increased recombination	UV–Vis/dye-loading analysis; EIS; spectral response; seal inspection	[20,36]
Elevated temperature	Sensitizer anchoring; solvent; seal; redox mediator; counter electrode; contacts/grid	V_{OC}/FF drift; diffusion changes; increased series resistance	Thermal cycling; FTIR/Raman; mass-loss analysis; EIS; contact/grid-resistance measurements	[20,36,59]
H_2O/O_2 ingress	TiO_2; sensitizer; electrolyte; seal; counter electrode/current collector	Non-uniform PCE decay; JSC/FF loss; catalytic/contact degradation	Hermeticity and humidity tests; microscopy; EIS; catalyst/compositional analysis	[49,51,59]
Electrical bias/redox cycling	Redox mediator; sensitizer oxidation state; catalyst; TCO/contact; metallic grid/interconnect	Bias-dependent degradation; FF loss; local current-collection loss	MPP light soaking; EIS; redox-speciation analysis; CV; grid/contact-resistance mapping	[25,37,60]

3. Intrinsic Molecular Instability of Sensitizers

3.1. Photochemical and Oxidative Decomposition

The sensitizer repeatedly cycles between its ground, excited, and oxidised states. A durable sensitizer must therefore withstand not only repeated photon absorption but also prolonged redox cycling without irreversible bond cleavage, radical coupling, or reaction with electrolyte species. Photochemical degradation can be promoted when sensitizer regeneration is slow because the oxidised state persists for longer periods, increasing the probability of competing side reactions. Sterically unprotected π-conjugated systems may also undergo aggregation at the oxide surface, altering excited-state pathways and promoting interfacial recombination. Modern sensitizer design increasingly considers photostability alongside light absorption and redox energetics. Recent studies emphasise donor–π–acceptor architecture, steric shielding, and anchoring-group optimisation as important molecular design parameters [26]. Primary studies involving copper-mediated systems further show that appropriate matching between the sensitizer and the redox mediator can support both high photovoltage and long-term device performance. A copper-modified bipyridine mediator combined with a tailored sensitizer retained 88% of its initial PCE after 95 days, illustrating the advantages of co-designing the sensitizer and its redox environment rather than optimising either component independently [61]. The 95-day result is therefore treated as Class B device-level stability evidence: it demonstrates durable photovoltaic operation, but the electrical retention metric alone does not directly establish molecular sensitizer stability.

3.2. Metal-Centre Instability in Macrocyclic Dyes

Metalloporphyrins and related macrocyclic sensitizers offer intense light absorption and highly tunable redox properties; however, the metal centre and its coordination environment introduce additional potential degradation pathways.

Changes in ligand–field interactions, axial coordination, nucleophilic attack, and reactions involving oxidised mediator species can modify the electronic structure even when

the macrocyclic chromophore remains structurally intact. Early high-efficiency porphyrin systems demonstrated the high photovoltaic performance achievable with cobalt-mediated architectures [5,6], while also highlighting the importance of steric shielding in limiting recombination between injected electrons and bulky metal-complex redox mediators.

Current molecular engineering continues to exploit this principle. Porphyrin sensitizers and copper-based redox complexes can be designed in combination to improve sensitizer-regeneration kinetics and suppress parasitic charge-transfer processes [62].

For long-term operation, metal-centre stability should be evaluated using post-ageing optical spectroscopy and electrochemical analysis, complemented where appropriate by additional chemical or structural characterisation techniques, rather than inferred solely from PCE retention. Changes in charge transport or recombination can partially mask molecular degradation at the device level, delaying its detection from photovoltaic performance parameters alone.

3.3. Chemical Degradation of Anchoring Groups

Anchoring groups determine both electronic coupling to the semiconductor and long-term retention of the sensitizer at the surface. Carboxylate anchoring groups are widely used because they provide straightforward adsorption and efficient electron injection; however, their binding equilibrium is sensitive to solvent composition, water content, temperature, and competing ionic species.

Desorption reduces the surface concentration of active sensitizer molecules and exposes previously covered TiO_2 sites to the electrolyte, which can simultaneously decrease J_{SC} and enhance interfacial recombination. Consequently, the resulting photovoltaic performance loss can be greater than would be expected from the reduction in optical absorption alone. Alternative anchoring groups and multiple-anchor molecular designs have been investigated to mitigate this process. Co-sensitisation using silyl- and carboxylate-anchored dyes has demonstrated that anchoring chemistry can be treated as an active molecular design parameter rather than merely as a means of attaching the sensitizer to the semiconductor [7].

More recently, cyano-rich sensitizer families have been explored as alternatives to conventional cyanoacrylic-acid-based anchoring motifs, with particular emphasis on adsorption stability and surface complex formation [63]. Accordingly, a decrease in J_{SC} should not be attributed directly to anchoring-group degradation unless sensitizer loss or altered surface binding is independently demonstrated. Stability studies should therefore quantify sensitizer loading before and after ageing and distinguish irreversible chemical degradation from reversible or competitive desorption.

3.4. Structure–Stability Relationships in Sensitizer Design

Structure–stability relationships are informed by two evidence streams that should not be conflated. Dedicated ageing studies can demonstrate retention or degradation directly, whereas studies of pyrazine sensitizers, co-sensitisation, tandem architectures, natural dyes, computational screening, and absorption prediction primarily establish how molecular structure affects light harvesting, electron injection, aggregation, or recombination [9,12,15–17,27,30,33,64–67]. The latter are therefore treated here as Class C design evidence with potential stability implications, not as demonstrated improvements in lifetime.

4. Interfacial Degradation at the Dye/TiO_2 Junction

4.1. Interfacial Desorption and Bond Weakening

The dye/TiO_2 junction is a dynamic chemical interface continuously exposed to light, ionic species, solvent, and elevated temperature. Even in the absence of irreversible sensitizer degradation, repeated protonation–deprotonation processes and competitive adsorption

can progressively weaken sensitizer–surface interactions. Thermal studies have shown that TiO_2 polymorphism and local surface structure can influence sensitizer retention as temperature increases [20]. In quasi-solid-state devices, polymer matrices can restrict molecular mobility and reduce sensitizer desorption; however, excessive polymer content may hinder ionic transport [68]. A useful mechanistic distinction can be made between primary sensitizer desorption and the secondary interfacial changes that follow.

Primary desorption directly reduces the surface coverage of active sensitizer molecules. Secondary degradation may occur when newly exposed TiO_2 sites interact with electrolyte cations or redox species, thereby modifying trap-state populations and increasing interfacial recombination.

This coupling explains why changes in optical absorbance alone may underestimate the electrical consequences of sensitizer loss. Post-ageing measurements of sensitizer loading or desorption should therefore be complemented by electrochemical impedance spectroscopy (EIS), transient electrical measurements, and surface-sensitive spectroscopic analysis. Accordingly, sensitizer desorption should be assigned as the dominant degradation mechanism only when changes in surface coverage or desorption are directly demonstrated, rather than inferred solely from photocurrent loss.

4.2. Surface Trap States and Recombination Enhancement

Recent interface-resolved ageing and co-adsorbent studies indicate that changes in the chemical composition of the sensitizer/electrolyte interfacial region and the occupation of exposed TiO_2 surface sites can directly modify recombination kinetics [52,69,70]. Trap states in nanostructured TiO_2 influence electron residence time, chemical capacitance, charge transport, and recombination. During ageing, trap-state populations may evolve through adsorption of electrolyte cations, proton insertion, surface contamination, and local structural reorganisation. Long-term photoelectrochemical studies have shown that the identity and size of electrolyte cations can alter trap-state density and shift the TiO_2 conduction-band edge [38]. Such changes may reduce photocurrent even when sensitizer absorption remains largely preserved. Ageing-induced photovoltaic changes are not necessarily monotonic. Impedance studies have reported a reduction in J_{SC} accompanied by an increase in V_{OC}, consistent with simultaneous changes in chemical capacitance, energetic alignment, and recombination behaviour [39]. These observations demonstrate that a single photovoltaic parameter cannot be used reliably to assign a unique degradation mechanism. Mechanistic diagnosis should therefore combine J–V characteristics with impedance-derived parameters such as recombination resistance, chemical capacitance, and electron lifetime, preferably measured under comparable illumination and electrical bias conditions.

4.3. Interfacial Chemical Reactions Under Ageing

Interfacial chemical reactions arise from the close proximity of oxidised sensitizers, semiconductor charge carriers, redox-active species, solvent molecules, and catalytic surfaces. Potential degradation pathways include solvent oxidation, ligand exchange, adsorption of decomposition products, and chemical modification of co-adsorbents. Because mesoporous photoanodes possess a very large internal surface area, even low-probability parasitic reactions can accumulate during prolonged operation.

An effective mitigation strategy is therefore to reduce the number of chemically accessible reactive sites while preserving electron injection and sensitizer regeneration. Compact or ultrathin passivation layers can limit direct electrolyte contact with conductive substrates and selected TiO_2 surface sites. A recent star-shaped block-copolymer overlayer nearly doubled the recombination resistance while maintaining mediator transport, demonstrating that soft interfacial layers can provide chemical protection without severely restricting ionic

accessibility [71]. Inorganic modification of TiO_2, including Fe/S incorporation, provides a complementary approach by modifying the optical and charge-transport properties of the photoanode [72]. Because several of these processes can produce similar electrical signatures, their assignment requires direct chemical or surface-sensitive evidence; changes in recombination resistance or PCE alone are insufficient to distinguish among solvent oxidation, ligand exchange, and adsorption of degradation products.

4.4. Ageing-Induced Modifications of Charge-Transfer Kinetics

Interface-engineering approaches based on compact layers, Ti^{3+}-modified TiO_2, MXene passivation, hybrid TiO_2/carbon structures, and tailored co-adsorbents illustrate the range of strategies currently available for reducing trap-mediated losses [70,73–77]. Ageing modifies the competition between electron injection, sensitizer regeneration, electron transport, and back-electron transfer. Because these processes occur on different timescales, a single structural or chemical change may affect J_{SC}, V_{OC}, and FF in different ways. For example, increased interfacial recombination can contribute primarily to a decrease in V_{OC}, whereas increased series resistance or restricted mediator diffusion can markedly reduce FF. Sensitizer loss directly reduces light harvesting and therefore J_{SC}, but the simultaneous exposure of previously covered TiO_2 sites can also enhance recombination. Data-driven degradation studies further support this multivariate interpretation. A study combining 400 fabricated DSSCs with finite-element simulations and long short-term memory modelling showed that TiO_2 thickness, porosity, sensitizer concentration, and iodine-electrolyte concentration interact non-linearly during device degradation [78]. These findings indicate that ageing behaviour cannot be adequately represented by a single stability constant. They also caution against direct ranking of different interface-engineering strategies when the underlying ageing conditions and diagnostic methods are not equivalent. A robust mechanistic assessment should instead follow the temporal evolution of multiple electrical parameters and correlate these changes with independent chemical or structural evidence. The coupled progression from operational stressors to elementary degradation processes and ultimately to device-level photovoltaic signatures is summarised schematically in Figure 2.

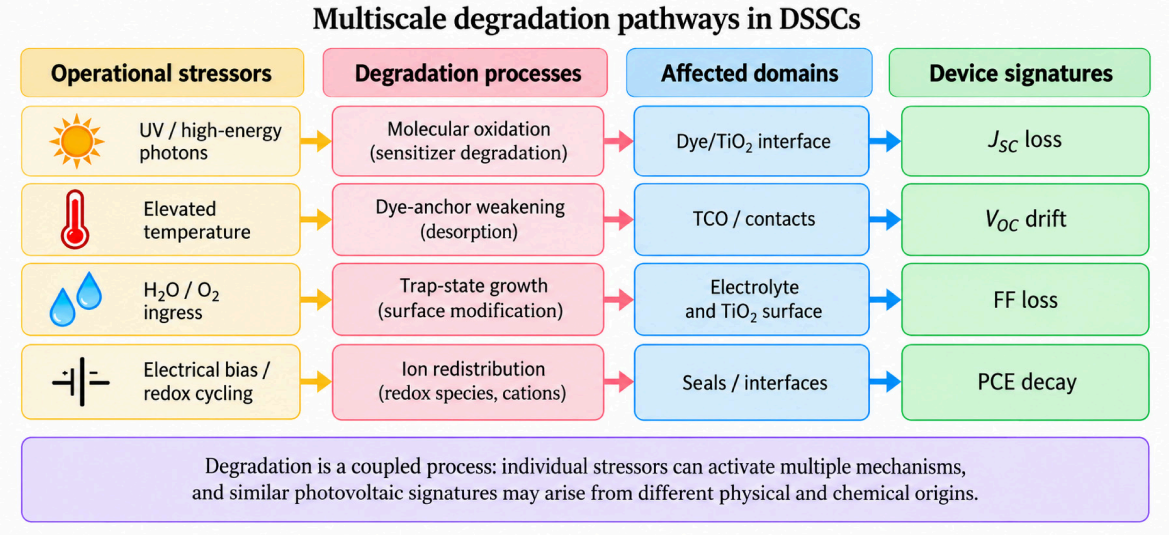


Figure 2. Multiscale representation of DSSC degradation linking operational stressors with degradation processes, affected device domains, and characteristic photovoltaic signatures. The pathways shown are representative and non-exclusive.

Table 2 highlights the strong coupling between sensitizer degradation and the chemistry of the dye/TiO_2 interface, as molecular instability can progressively alter surface cover-

age, trap-state populations, and recombination kinetics. Consequently, stability-oriented sensitizer design should be integrated with robust anchoring and interfacial passivation strategies rather than focused exclusively on light absorption and initial PCE.

Table 2. Major sensitizer and dye/TiO_2 interfacial degradation pathways and corresponding stability-oriented strategies.

Degradation Mechanism	Main Consequences	Stability-Oriented Response	References
Photo-oxidation/ irreversible sensitizer degradation	Reduced light absorption and electron injection Additional recombination pathways	Steric shielding Rapid sensitizer regeneration Sensitizer–mediator matching	[26,61,62]
Anchoring-group weakening/ sensitizer desorption	Reduced sensitizer loading Exposure of TiO_2 surface sites J_{SC} loss	Multiple or alternative anchoring groups Controlled surface chemistry	[7,20,63]
Trap-state evolution	V_{OC} variation Reduced electron lifetime Enhanced recombination	Surface passivation Control of cation adsorption Compact interlayers	[38,79]
Interfacial parasitic reactions	Increased interfacial resistance Coupled changes in J_{SC}, V_{OC} and FF	Ultrathin interlayers Polymer or oxide passivation	[71,72]

5. Degradation of Charge Collectors, Counter Electrodes, and Metallic Interconnects

5.1. Structural and Morphological Changes in TCO Substrates

Transparent conducting oxides (TCOs) are often treated as chemically and electrically inert current collectors; however, their morphology, thermal history, and chemical composition can influence both device fabrication and long-term stability. Fluorine-doped tin oxide (FTO) generally tolerates the high-temperature processing steps used for TiO_2 sintering and counter-electrode preparation better than indium tin oxide (ITO) and zinc-oxide-based conductors. Comparative studies of FTO, ITO, aluminium-doped zinc oxide (AZO), and gallium-doped zinc oxide (GZO) have shown that FTO exhibits greater thermal and chemical robustness under representative counter-electrode processing conditions [40].

During operation, local heating, electrolyte exposure, and mechanical stresses can alter the electrical contact at the TCO/porous-layer interface. Microcracks, interfacial defects, or poorly adhered layers may not immediately cause catastrophic failure; instead, they can contribute to a gradual increase in series resistance and a corresponding reduction in fill factor. For this reason, sheet resistance should be measured before device fabrication and after ageing, while cross-sectional or surface microscopy can help distinguish changes within the TCO from interfacial delamination or contact degradation. Accordingly, a decrease in fill factor or an increase in series resistance should not be considered direct evidence of TCO degradation unless supported by independent conductivity or morphological measurements.

5.2. Electrochemical Corrosion of ITO and FTO

Iodide/triiodide and alternative redox mediators can be chemically aggressive towards metallic grids, catalytic materials, and less stable conducting oxides. FTO is comparatively robust, but it should not be regarded as universally inert: pinholes in compact layers, edge

exposure, or defects in protective coatings can create locally aggressive electrochemical environments. ITO is generally more sensitive to thermal processing and may undergo conductivity changes that can be difficult to distinguish from electrolyte-induced degradation [40]. A stability-oriented device design should therefore minimise direct electrolyte contact with the transparent conductor wherever possible. Dense TiO_2 compact layers are particularly useful because they can suppress recombination at the FTO/electrolyte interface while simultaneously providing a physical barrier against direct electrolyte exposure. Recent compact-layer engineering using combined chemical-bath deposition and spray-pyrolysis approaches improved device performance under both one-sun and low-light conditions, demonstrating the electrical benefits of isolating the collector from the electrolyte [67]. Long-term studies should additionally determine whether these improvements are retained after combined thermal and chemical ageing. Because thermal degradation and electrolyte-induced corrosion can produce similar electrical consequences, corrosion should be assigned only when chemical, morphological, or conductivity evidence confirms deterioration of the conductive substrate.

5.3. Ion Diffusion and Conductivity Loss

Ion migration can affect the conductive network indirectly even when the TCO itself remains structurally intact. Iodine-containing species, protons, alkali-metal cations, and electrolyte decomposition products can accumulate near interfaces, modify local potential distributions, and alter interfacial contact chemistry. In large-area DSSC modules, redistribution of iodine species can become spatially non-uniform, leading to uneven current collection and progressive performance degradation. A 12-year outdoor module study provides evidence over a practically relevant timescale: hydrophobic additives were combined with module architectures designed to suppress biased iodine redistribution, resulting in improved long-term durability [49]. Although this study provides unusually long-term evidence, its outcome should not be directly compared with accelerated laboratory tests because ion redistribution and current-collection losses depend strongly on module geometry, electrical bias, temperature history, and exposure conditions.

This finding indicates that ion-management strategies should be considered alongside conventional conductivity measurements. Spatially resolved techniques, such as local sheet-resistance mapping or current-distribution imaging, can reveal degradation patterns that may remain undetected in a single global J–V characteristic.

5.4. Impact on Charge Collection and Series Resistance

Degradation of charge collection typically manifests as increased series resistance, reduced fill factor, and, at more advanced stages, a decrease in J_{SC}. However, series resistance is distributed across several device components, including the TCO, electrical contacts, porous-semiconductor transport pathways, counter-electrode interfaces, and electrolyte-diffusion processes. Assigning a measured resistance increase exclusively to the TCO on the basis of J–V characteristics alone is therefore unreliable.

Electrochemical impedance spectroscopy (EIS) can help separate these contributions when equivalent-circuit analysis is interpreted in the context of the specific device architecture. Ageing studies have associated an overall increase in resistance with photocurrent loss while simultaneously observing changes in recombination behaviour and chemical capacitance [39].

For the assessment of conductive-layer degradation, EIS should therefore be combined with four-point-probe measurements, TCO optical-transmission measurements, contact-resistance analysis, and appropriate microscopic characterisation. The objective is not only to

preserve low initial sheet resistance but also to maintain stable lateral and through-thickness charge collection throughout device ageing.

5.5. Counter-Electrode Catalyst and Metallic-Grid Degradation

Counter-electrode degradation is a distinct failure location from TCO or front-contact degradation and therefore requires different diagnostics. In conventional iodide/triiodide DSSCs, platinum can lose catalytic activity through dissolution, detachment, or poisoning by redox or electrolyte species, whereas alternative carbon, polymer, and transition-metal catalysts may undergo oxidation, phase changes, or loss of adhesion [59]. Such changes are best resolved using symmetric-cell or full-cell EIS, cyclic voltammetry, catalytic-surface microscopy, and compositional analysis rather than by assigning a fill-factor loss to the TCO. Module-scale current collectors introduce an additional reliability constraint. Silver grids reduce ohmic losses in large-area parallel modules but can be corroded by iodide-containing electrolytes; replacement with more corrosion-resistant collectors or complete barrier coverage can therefore improve durability.

A platinum-grid module, for example, retained an AM1.5 efficiency of 4.1% after 1700 h while avoiding the grid corrosion observed in silver-based structures [60]. These observations show why catalyst ageing, TCO degradation, and grid/interconnect corrosion should be reported as separate mechanisms even when all three ultimately manifest as increased series resistance or reduced fill factor.

6. Electrolyte-Induced Degradation Pathways

6.1. Volatility, Solvent Evaporation, and Leakage

Liquid electrolytes provide efficient pore filling and high ionic mobility but remain a major source of extrinsic instability in DSSCs. Solvent evaporation alters mediator concentration and electrolyte viscosity, whereas leakage decreases the available electrolyte volume and can expose regions of the porous electrode. These processes can simultaneously affect ionic diffusion, sensitizer regeneration, and counter-electrode kinetics. The stability challenge is particularly pronounced for volatile nitrile-based solvents, which provide high ionic conductivity but also exhibit relatively high vapour pressure and therefore require effective sealing strategies [24].

Several recent approaches aim to reduce this vulnerability while retaining liquid-like ion transport. The titanium-based metal–organic framework MIL-125 can immobilise iodide/triiodide electrolyte within its porous structure while maintaining effective ionic transport; the optimised system retained approximately 75% of its initial PCE after 1400 h [80].

Aerogel-based electrolyte encapsulation provides a related porous-retention strategy and showed a smaller efficiency decrease than a conventional liquid-electrolyte cell over a two-year comparison [81]. These outcomes should not be compared directly because the reported devices differ in architecture, electrolyte formulation, exposure duration, and ageing conditions. Their common significance lies instead in demonstrating that electrolyte confinement can reduce volatility-related losses while preserving sufficient ionic transport. These approaches shift the stability challenge from a simple distinction between liquid and solid electrolytes towards the effective confinement of a mobile redox phase. Recent studies of liquid, aqueous, quasi-solid, and polymer-gel electrolytes further demonstrate that solvent volatility, ionic conductivity, and electrolyte retention should be optimised simultaneously rather than considered independently [47,55,56,82–85].

6.2. Redox-Couple Instability (I^-/I^{3-}, Cobalt, and Copper Systems)

The iodide/triiodide redox couple remains a widely used benchmark because of its favourable regeneration kinetics; however, it absorbs part of the visible spectrum, limits

the attainable photovoltage, and can promote corrosion of metallic components. Cobalt- and copper-based redox complexes can provide more positive redox potentials and higher V_{OC} values, but their larger molecular dimensions and ligand-dependent chemistry make diffusion and chemical compatibility more sensitive to solvent composition, additives, sensitizer structure, and catalyst selection [25,86].

The development of asymmetric copper redox mediators illustrates how coordination chemistry can be engineered to reduce recombination while maintaining efficient sensitizer regeneration, enabling a reported PCE of 35.6% under 1000 lx warm-white compact-fluorescent-lamp illumination [87]. A copper-modified bipyridine mediator further demonstrated that improved chemical stability and reduced sensitivity to additive-induced deactivation can be incorporated into the redox complex itself, with 88% of the initial PCE retained after 95 days [61]. These results represent complementary rather than directly comparable outcomes: high indoor PCE reflects favourable energetic and kinetic matching, whereas long-term PCE retention provides information on device-level chemical and interfacial durability. Together, they support treating the redox mediator as a molecularly engineered interfacial partner rather than as an interchangeable electrolyte component. Recent studies of additive coordination, aqueous copper electrolytes, and thiocyanate-free sensitizer/mediator combinations further emphasise chemical compatibility as a key criterion for long-term stability [54,56,58,88].

6.3. Chemical Decomposition in Ionic-Liquid and Gel Electrolytes

Replacing volatile solvents with gelled, ionic-liquid, or polymer-based electrolytes can substantially reduce leakage and solvent loss but introduces additional stability constraints, including polymer swelling, phase separation, crystallisation, additive immobilisation, and reduced ionic diffusivity.

Poly(methyl methacrylate) (PMMA)-based quasi-solid electrolytes demonstrate that polymer composition and salt ratio strongly influence ionic conductivity and thermal stability; improved long-term performance retention can be achieved even when the initial PCE remains lower than that of a corresponding liquid-electrolyte reference [89,90].

Studies based on poly(vinylidene fluoride-co-hexafluoropropylene) (PVDF-HFP) similarly indicate that polymer molecular weight and sensitizer compatibility can influence both charge transport and long-term sensitizer retention [68].

Solid polymer electrolyte films eliminate volatile solvents entirely. Systems based on poly(ethylene oxide) (PEO), poly(ethylene glycol) (PEG), and TiO_2 achieved PCE values above 8% while retaining approximately 98% of their initial efficiency after 700 h, demonstrating that solvent-free ionic conduction is feasible when pore infiltration and interfacial contact are adequately maintained [91].

However, this retention value should be interpreted within the specific test protocol and device architecture, because polymer content, pore infiltration, temperature, and electrical operating conditions strongly influence the balance between ionic transport and long-term stability. Printable and in situ-gelled copper-electrolyte systems extend this approach towards manufacturable indoor photovoltaic devices, where direct-contact architectures can shorten ion-transport distances and improve low-light performance [92,93].

Additional electrolyte concepts include biopolymer-based gels, polyacrylonitrile (PAN)/PEG matrices, covalent organic framework (COF)-assisted liquid electrolytes, and data-driven electrolyte-formulation screening, thereby expanding the design space between conventional liquid electrolytes and fully solid-state systems [82–84,94,95].

6.4. Electrolyte-Driven Corrosion and Secondary Reactions

Electrolyte degradation products can react with counter-electrode catalysts, metallic current collectors, sensitizers, and sealing materials. Conversely, corrosion or decomposition products generated at these components can contaminate the electrolyte or modify catalytic kinetics, creating coupled degradation feedback. Such secondary processes are difficult to identify solely from PCE decay because the initial degradation event may originate in one component while the dominant late-stage resistance develops elsewhere in the device. Reducing solvent volatility is therefore necessary but not sufficient for long-term electrolyte stability. The electrolyte must remain chemically compatible with the entire device stack. Deep eutectic-solvent (DES)-like iodide electrolytes combine low volatility and reduced flammability with redox functionality; a 2024 system retained approximately 95% of its initial performance for more than two months [96]. This result is therefore treated as Class B evidence of device durability; attribution of the improvement specifically to suppressed electrolyte-driven corrosion would require independent chemical or interfacial diagnostics. More recently, sensitizers incorporating glycerol- or ethylene-glycol-like side chains were specifically matched with neat DES electrolytes, improving both indoor photovoltaic performance and multi-month stability [97].

This type of sensitizer–electrolyte co-design provides a useful strategy for reducing secondary reactions through improved local chemical compatibility.

The representative outcomes listed in Table 3 were obtained under different device architectures and testing conditions and should not be interpreted as directly comparable quantitative stability metrics. The table nevertheless highlights the persistent trade-off between electrolyte stability and ionic transport: reducing volatility and leakage can increase viscosity, limit pore infiltration, or introduce additional interfacial resistance. Recent strategies therefore aim to retain efficient redox transport while immobilising, confining, or replacing the volatile solvent phase, as demonstrated by gel, MOF-assisted, DES-based, copper quasi-solid, and solid-polymer electrolyte systems.

Table 3. Electrolyte-engineering strategies, representative device outcomes, and evidence for DSSC stability.

Electrolyte Strategy	Device/Test Context	Representative Outcome	Evidence Class	References
Conventional liquid electrolyte	Benchmark liquid-electrolyte DSSCs; strongly dependent on solvent volatility and sealing	High ionic transport, but volatility and leakage remain major lifetime constraints	Context only	[24]
PVDF-HFP gel electrolyte	Z907/N719/phenothiazine quasi-solid DSSCs; >600 h ageing, including 70 °C and 40–45% RH	Polymer molecular weight affects JSC retention and ion-transport losses; no single formulation is universally superior	B	[68]
PEO/PEG/TiO_2 solid polymer film	Solvent-free solid-state DSSC; initial PCE up to 8.13%; 700 h test	98% of initial efficiency retained after 700 h	B	[91]
MIL-125-assisted quasi-solid electrolyte	AM1.5G, 100 mW cm^{-2}; ~23 °C; 1400 h; leakage/conductivity and EIS assessed	~75% of initial PCE retained after 1400 h; indoor PCE of 27.6% at 6000 lx is a separate performance metric	A	[80]

Table 3. *Cont.*

Electrolyte Strategy	Device/Test Context	Representative Outcome	Evidence Class	References
DES/DES-like electrolyte	Non-V_{OC} iodide medium; >2-month temporal test; low-light and outdoor performance also reported	~95% of initial performance retained for >2 months; suppression of corrosion was not independently demonstrated	B	[96,97]
Copper gel/direct-contact architecture	Indoor performance study using direct-contact/in situ gelation; no equivalent long-term test in the cited record	Indoor PCE > 35–36%; this is a performance result, not lifetime evidence	C	[92,93]

Evidence classes: A = ageing studies supported by independent mechanistic diagnostics in addition to photovoltaic measurements; B = device-level retention or ageing studies without independent confirmation of the dominant degradation mechanism; C = performance/design studies without dedicated ageing evidence. "Context only" denotes general contextual evidence not assigned to Classes A–C.

7. Surface and Interface Engineering Strategies for Stability Enhancement

7.1. TiO_2 Surface Passivation and Interlayers

Passivation strategies aim to reduce electronically and chemically active surface sites without significantly hindering electron injection or redox-mediator transport. Compact TiO_2 layers at the FTO/photoanode interface can limit direct FTO/electrolyte contact and suppress interfacial recombination, while ultrathin organic or inorganic coatings can reduce back-electron transfer at the sensitized mesoporous TiO_2 surface.

Recent compact-layer engineering achieved PCE values of 9.86% under one-sun illumination and 29.68% at 200 lux, illustrating the benefits of interface control under both standard and low-light operating conditions [79]. Soft passivation layers provide an alternative approach. A star-shaped polystyrene-block-PMMA overlayer increased recombination resistance while maintaining redox-species transport towards the sensitizer/electrolyte interface [71]. Bio-derived modification offers another route: lignin-modified TiO_2 improved porosity, sensitizer adsorption, and thermal protection, with a photoanode containing 5% lignin retaining 78% of its initial PCE after 90 days [98].

These results show that passivation need not rely exclusively on dense inorganic barriers but can also be achieved through chemically tailored interphases. Recent studies using MXene-based interfacial layers, Ti^{3+}-rich TiO_2, hybrid TiO_2/carbon photoanodes, and molecular co-adsorbents further demonstrate that interfacial modification can influence surface morphology, recombination resistance, electron lifetime, and sensitizer loading [70,74–77].

Because these approaches were evaluated using different device architectures, illumination conditions, and stability metrics, their reported benefits should be interpreted mechanistically rather than as directly comparable performance rankings.

7.2. Protective Coatings for Conductive Substrates

Protective coatings applied to TCO substrates can serve two complementary functions: reducing parasitic charge transfer and physically isolating the conductive substrate from chemically aggressive electrolyte species.

Dense TiO_2 underlayers represent a widely used example, although the same principle can be extended to chemically resistant oxide, polymeric, or hybrid coatings, provided that optical transmission and lateral electrical conductivity are preserved. The choice of

protective layer should also account for the thermal sensitivity of the underlying conductor, as ITO and zinc-oxide-based TCOs are generally less tolerant of high-temperature processing than FTO [40].

A stability-oriented protective coating should also maintain its integrity and adhesion during thermal cycling. Thin barrier layers that crack or delaminate may promote localised corrosion by concentrating ionic current at defects. Consequently, coating evaluation should include adhesion, pinhole density, electrochemical leakage current, and post-ageing microscopic analysis in addition to initial J–V performance.

An integrated approach in which TCO protection is combined with photoanode compact-layer engineering can simultaneously improve charge collection and reduce direct chemical exposure of the conductive substrate.

7.3. Barrier Layers and Encapsulation Strategies

Encapsulation is essential for distinguishing intrinsic material degradation from failure caused by environmental ingress or electrolyte loss. Polymeric seals are convenient and compatible with relatively low-temperature processing, but they may allow gradual solvent diffusion and the ingress of oxygen and moisture during prolonged operation. Glass-frit sealing provides substantially lower permeability, although conventional high-temperature processing can adversely affect sensitizers and electrolyte components.

Laser-assisted, ultralow-temperature glass-frit sealing reduced the processing temperature to approximately 110 °C and produced iodide- and cobalt-mediated devices that remained stable for 1000 h under the ISOS-L-2 light-soaking ageing protocol [99].

A particularly challenging aspect of encapsulation is the hermetic sealing of electrolyte-filling openings. Fully glass-encapsulated cells incorporating laser-structured capillary-like filling holes passed helium-leak and humidity-freeze tests and maintained their PCE after more than 4300 h of accelerated ageing [51]. Fully glass-encapsulated cobalt-mediated monolithic DSSCs similarly retained or improved their photovoltaic performance under several ageing conditions [50].

These results are not directly comparable in quantitative terms because the devices and ageing protocols differ, but together they provide consistent evidence that improved hermeticity can substantially reduce package-related failure and reveal the intrinsic stability of the active device chemistry.

These studies demonstrate that encapsulation is not merely a manufacturing consideration but an important experimental variable that determines whether the observed degradation is predominantly extrinsic or intrinsic. Device-level reliability studies further indicate that appropriate sealing, electrolyte immobilisation, and device architecture can improve stability during prolonged illumination and elevated-temperature operation, including mini-module configurations relevant to Internet of Things (IoT) power supplies [21,47,100].

7.4. Hydrophobic and Anti-Corrosion Surface Modifications

Hydrophobic surface modification is particularly attractive because it can reduce water interaction at the molecular and interfacial levels even when the external encapsulation is not perfectly impermeable. Long-chain benzimidazole additives can passivate TiO_2 surfaces and reduce their susceptibility to water-induced degradation.

Their long-term effectiveness has been demonstrated in DSSC modules that remained operational after 12 years of outdoor exposure [49]. This long-term outdoor evidence is particularly valuable, although the observed durability reflects the combined effects of surface modification, module architecture, and realistic environmental exposure rather than the isolated contribution of hydrophobic passivation alone.

Related approaches include hydrophobic sensitizer substituents and electrolyte-compatible side chains designed to reduce local water activity while maintaining sufficient ionic transport. Anti-corrosion strategies should also minimise direct galvanic or redox-active contact between chemically aggressive mediator species and susceptible metallic components. Carbon-based catalysts, protective TCO interlayers, and chemically resistant current collectors can reduce this risk. Importantly, both hydrophobic protection and corrosion resistance should be evaluated after thermal cycling because surface segregation, additive redistribution, or interfacial migration may diminish the initial protective effect.

Durable surface engineering therefore requires not only favourable chemical interactions but also the long-term spatial stability of protective species within the device architecture. The complementary roles of molecular protection, interface passivation, electrolyte retention, conductor protection, and encapsulation are summarised in the integrated stability-engineering framework shown in Figure 3.

The representative indicators listed in Table 4 were obtained under different device architectures, stress conditions, and evaluation protocols and should not be interpreted as directly comparable measures of stability or performance. As summarised in Table 4, no single protective strategy can address all DSSC degradation pathways simultaneously. Long-term stability therefore depends on combining surface passivation, corrosion control, electrolyte retention, and effective encapsulation so that improvements at one interface are not offset by degradation elsewhere in the device stack.

Table 4. Surface, interface, and encapsulation strategies, representative outcomes, and evidence for DSSC stability.

Strategy	Device/Ageing Context	Representative Outcome	Evidence Class	References
Hydrophobic TiO_2 passivation	Outdoor DSSC module under combined realistic stresses; 12 years	~75% of initial performance retained; durability reflects passivation together with module design and ion management	B	[49]
Lignin-modified TiO_2	5% lignin photoanode; 90-day ageing; electrical tracking with structural rationale	78% of initial PCE retained after 90 days	B	[98]
Compact TiO_2 layer	Y123/Co^{2+} /$^{3+}$ DSSC; AM1.5G and 200 lx room light; SEM/EIS characterisation	9.86% at one sun; 24.74% for a single cell and 29.68% for a tandem device at 200 lx; no dedicated lifetime test	C	[79]
Star-shaped block-copolymer interlayer	Interface/passivation study with EIS-based recombination analysis	Nearly twofold increase in recombination resistance; stability implication remains design-level without long-term ageing	C	[71]
Full glass-frit sealing	Fully glass-sealed DSSC; ISOS-L-2/3 ageing plus helium-leak and IEC 61646 humidity–freeze testing	PCE maintained after 4336 h of accelerated ageing; package hermeticity independently verified	A	[51]
Aerogel-based electrolyte encapsulation	Aerogel-confined liquid electrolyte; two-year comparison with a conventional liquid-electrolyte cell	Smaller efficiency loss than the liquid reference after two years; improved electrolyte retention	B	[81]

Evidence classes: A = ageing studies supported by independent mechanistic diagnostics in addition to photo-voltaic measurements; B = device-level retention or ageing studies without independent confirmation of the dominant degradation mechanism; C = performance/design studies without dedicated ageing evidence.

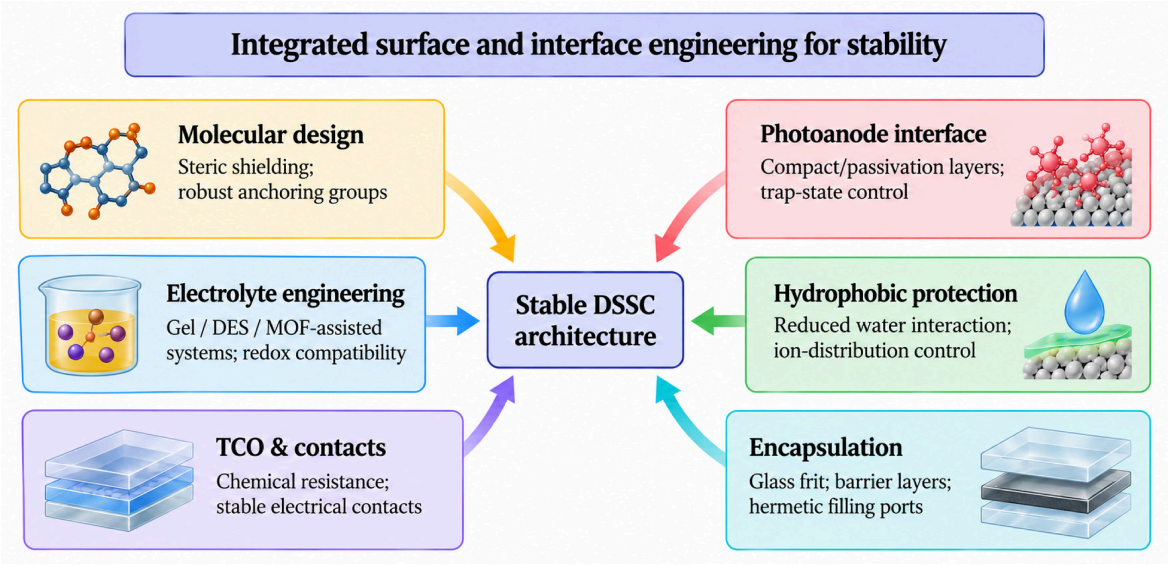


Figure 3. Integrated surface- and interface-engineering framework for improving DSSC stability. Long-term durability requires coordinated molecular design, interface passivation, electrolyte management, conductor protection, hydrophobic modification, and effective encapsulation rather than reliance on a single protective strategy.

8. Stability Evaluation and Ageing Methodologies

8.1. Accelerated Ageing Protocols

Accelerated ageing protocols should reproduce the dominant stressors associated with the intended application while reducing the required observation time without introducing unrealistic failure mechanisms. Classical DSSC stability studies employed elevated-temperature storage, full-sun light soaking, and combined thermal–illumination exposure to distinguish thermally activated degradation from photoinduced processes [36].

More recent studies increasingly control illumination, temperature, and electrical operating conditions; however, substantial heterogeneity between testing procedures remains. A meaningful accelerated-ageing matrix should include dark thermal storage, continuous light soaking, combined temperature and illumination exposure, humidity testing, and electrical operation under representative load conditions, preferably near the maximum power point. Initial and periodic J–V measurements should be complemented by electrochemical impedance spectroscopy (EIS) and at least one chemically or structurally sensitive diagnostic method.

Ageing duration alone is insufficient to describe the applied stress: cumulative photon exposure, temperature history, humidity conditions, and electrical operating state should also be reported to improve comparison of degradation behaviour across laboratories. Accordingly, accelerated-ageing results should be interpreted in terms of the applied stress history rather than test duration alone, particularly when comparing studies performed under different illumination, thermal, or electrical conditions.

8.2. Light-Soaking and Thermal-Cycling Tests

Recent ageing studies range from interface-resolved spectroscopic investigations under illumination to year-scale ambient-light exposure and 1000 h module-level operation, illustrating the importance of combining accelerated testing with application-relevant stress conditions [47,56,66,69,100]. Light soaking probes the device under a coupled photoelectrochemical operating state and should therefore be described in terms of illumination spectrum, irradiance, temperature, and electrical boundary condition. Thermal cycling

introduces repeated expansion and contraction, together with temperature-dependent changes in electrolyte distribution and transport, and can therefore reveal sealing or contact degradation that may remain undetected during isothermal storage. The pronounced influence of the external-circuit condition during 1000 h light-soaking experiments demonstrates why operation near the maximum power point or under a representative electrical load is more informative than an unspecified open-circuit condition [37].

Module-relevant testing should also include post-cycle hermeticity assessment and spatially resolved inspection where appropriate. Glass-encapsulated DSSCs have successfully undergone humidity–freeze and related reliability tests, while long-term outdoor studies demonstrate the additional importance of ion redistribution and realistic diurnal temperature variations [49,51].

An effective accelerated test should therefore reproduce the dominant degradation mechanisms expected under the intended operating conditions rather than merely impose the most severe possible stress.

8.3. ISOS Protocols and Their Applicability to DSSCs

The original International Summit on Organic Photovoltaic Stability (ISOS) consensus protocol, published by Reese et al. in 2011 and developed from the first three ISOS meetings, defines test families for dark or shelf storage, outdoor exposure, laboratory light soaking/weathering, and thermal cycling, with three levels of experimental control [101]. ISOS procedures are comparison and reporting protocols rather than pass/fail qualification standards. Later consensus work on perovskite photovoltaics retained this stress-specific logic and further emphasised maximum-power-point operation, encapsulation reporting, and the separation of single-stressor from combined-stressor experiments [102].

For DSSCs, an ISOS designation should be accompanied by device-specific information because liquid and quasi-solid electrolytes introduce variables that are less relevant to dry thin-film devices. In particular, electrolyte composition and volume, filling-port design, seal chemistry, active area, counter electrode, and electrical operating state should be reported. The fully glass-sealed DSSCs discussed in this review were aged for 4336 h using ISOS-L-2/3 light-soaking procedures and were separately subjected to helium-leak and IEC 61646 humidity–freeze testing [51]. These tests should not be placed on a single lifetime axis: light soaking probes photoelectrochemical operation; elevated-temperature dark storage probes thermally activated chemistry; outdoor exposure combines variable spectral, temperature, humidity, and load histories; and IEC-type humidity–freeze testing is a qualification-oriented package stress rather than an operational-lifetime measurement. Where the source provides this information, studies should also state whether J–V measurements were obtained in situ during ageing or after a recovery/equilibration period, because reversible ion redistribution and temperature-dependent transport can otherwise be mistaken for permanent degradation.

8.4. Limitations of Current Testing Approaches

Cross-study comparison remains challenging because recent DSSC reports employ full-sun, low-light, thermal-storage, dark-storage, and continuous-illumination tests with different retention metrics, sampling intervals, and reporting conventions [47,48,56,66,69,85,100]. A major limitation of the current literature is therefore methodological heterogeneity.

Reported studies differ in active area, encapsulation method, illumination spectrum, temperature, test duration, sampling frequency, and data-normalisation procedures. Some report only PCE retention, whereas others monitor the evolution of individual photovoltaic parameters and impedance-derived quantities.

These differences limit reliable quantitative comparison and may create an apparent superiority of one material system or device architecture when the underlying testing conditions are not equivalent. A further limitation is the frequent absence of independent mechanistic verification. A decrease in PCE may be attributed to sensitizer degradation, electrolyte loss, or increased recombination without direct chemical, structural, or interfacial evidence. Data-driven studies demonstrate the value of large time-resolved datasets and quantitative degradation metrics [66].

Future stability protocols should therefore distinguish between performance retention and mechanistic stability and should incorporate at least one independent diagnostic measurement capable of supporting the proposed degradation pathway.

Table 5 emphasises that meaningful comparison of DSSC stability depends not only on device chemistry but also on consistent and sufficiently detailed reporting. Without a complete description of the device architecture, applied stress conditions, electrical-performance evolution, and mechanistic diagnostics, reported stability improvements cannot be reliably compared across laboratories or transferred between device architectures.

Table 5. Recommended minimum reporting requirements for DSSC stability studies.

Category	Minimum Information	Why It Matters	References
Device definition	Active area Substrate/TCO TiO_2 thickness Sensitizer Redox mediator Solvent or gel electrolyte Counter electrode Sealing method Electrolyte volume	Prevents differences in device architecture from being incorrectly attributed to material chemistry	[36,47,78]
Stress conditions	Illumination spectrum and irradiance Temperature Relative humidity Test duration Thermal cycling conditions Electrical operating state	Defines the applied environmental and electrical stress and facilitates comparison between studies	[20,36,37,50]
Electrical tracking	J_{SC}, V_{OC}, FF, PCE at defined intervals Maximum power point (MPP) operation where appropriate	Distinguishes current-, voltage-, and resistance-related degradation trends	[36,47,78,100]
Mechanistic diagnostics	EIS combined with at least one independent chemical, spectroscopic, structural, or surface-sensitive method	Provides independent evidence supporting the proposed degradation mechanism	[38,39,52,69]
Post-ageing assessment	Sensitizer loading/absorption Seal inspection Mass change or hermeticity testing TCO/contact resistance	Helps distinguish reversible redistribution processes from permanent material or interface degradation	[47,49,51,69]

9. Linking Performance Decay to Degradation Mechanisms

9.1. Evolution of J_{SC}, V_{OC}, and Fill Factor During Ageing

The short-circuit current density (J_{SC}) is particularly sensitive to changes in light harvesting, sensitizer coverage, electron-injection efficiency, charge collection, and redox-

mediator diffusion. The open-circuit voltage (V_{OC}) is governed primarily by the TiO_2 electron quasi-Fermi level and interfacial recombination kinetics, whereas the fill factor (FF) is strongly influenced by series resistance, counter-electrode kinetics, ionic diffusion, and shunt pathways. Ageing can therefore produce non-intuitive combinations of photovoltaic changes. For example, aged devices may exhibit a decrease in J_{SC} accompanied by an increase in V_{OC} when changes in energetic alignment and charge-transfer behaviour occur simultaneously [39].

Monitoring the temporal evolution of individual photovoltaic parameters is more informative than comparing only the initial and final PCE values. A progressive decrease in J_{SC} with relatively stable V_{OC} may indicate loss of sensitizer, reduced injection efficiency, diffusion limitations, or impaired charge collection, whereas simultaneous decreases in V_{OC} and FF may indicate enhanced interfacial recombination and/or increasing resistive losses. A pronounced decrease in FF after an initially stable period can also indicate electrolyte depletion, contact degradation, seal failure, or deterioration of counter-electrode kinetics. Such interpretations should be treated as mechanistic hypotheses until they are supported by complementary measurements such as EIS, spectroscopy, or physical inspection.

Recent studies combining impedance analysis, interface-sensitive characterisation, and device-level stability monitoring demonstrate that similar PCE losses can arise from different combinations of recombination, transport limitations, sensitizer modification, and electrolyte evolution [48,52,57,66,69,70].

9.2. Efficiency–Stability Trade-Offs

These values should not be interpreted as a direct ranking of stability because the corresponding devices differ in electrolyte chemistry, encapsulation, architecture, and ageing protocol. Their value is therefore comparative at the level of design trade-offs rather than as directly comparable lifetime metrics.

For indoor applications, the balance between efficiency and stability differs because irradiance levels are lower and device temperatures are generally more moderate. High photovoltage and favourable spectral matching can partly compensate for lower absolute photocurrent, making quasi-solid copper-mediated systems particularly relevant for low-light operation [87,92,93]. Stability targets should therefore be defined according to the intended application rather than by a single universal PCE-retention threshold.

9.3. Identification of Dominant Degradation Pathways

Dominant degradation pathways can be identified by combining characteristic photovoltaic trends with targeted diagnostic measurements. Sensitizer loss can be supported by reduced optical absorption or dye-loading measurements; electrolyte loss by mass change, visible void formation, or changes in electrolyte composition; increased recombination by reduced recombination resistance and shorter electron lifetime; TCO/contact degradation by changes in sheet resistance and series resistance; and sealing failure by hermeticity or moisture-ingress testing. The objective is to establish a causal sequence linking the applied stressor to a measurable physical or chemical change and, ultimately, to its electrical consequence.

Because degradation mechanisms interact, the dominant pathway may change during ageing. A device may initially undergo slow sensitizer desorption, followed by enhanced recombination at newly exposed TiO_2 surface sites, subsequent changes in electrolyte composition, and deterioration of catalytic activity.

Machine-learning approaches can assist in identifying such nonlinear transitions when sufficiently detailed time-series datasets are available [78]. However, predictive models are

most useful when they incorporate physically interpretable variables and are supported by independent diagnostic measurements.

Data-driven electrolyte optimisation and device-level modelling further demonstrate how multivariate approaches can be linked to physically meaningful descriptors rather than used solely as empirical predictors [48,94].

Table 6 converts photovoltaic signatures into an evidence hierarchy for mechanism assignment. Electrical trends remain useful for identifying a likely failure domain, but a degradation mechanism is treated as directly supported only when an independent chemical, structural, electrochemical, microscopic, spectroscopic, or package-level measurement confirms the affected component or process. This approach reduces the risk of assigning similar J–V changes to different mechanisms without sufficient evidence.

Table 6. Evidence-based assignment of representative DSSC degradation mechanisms.

Degradation Mechanism	Independent Evidence for Direct Assignment	Common Photovoltaic Signature	Evidence Assessment	References
Sensitizer loss/desorption	Post-ageing dye-loading or desorption analysis; UV–Vis/FTIR or other surface-sensitive spectroscopy	JSC loss; possible VOC change as TiO_2 sites become exposed	Class A requires direct measurement of sensitizer loss or altered binding; electrical decay alone remains Class B inference	[20,63,69]
TiO_2 trap-state/recombination evolution	EIS-derived chemical capacitance, recombination resistance, and electron lifetime, complemented where possible by surface/interfacial analysis	VOC drift; JSC/VOC changes that may be non-monotonic	EIS combined with interface-sensitive evidence can support Class A assignment; J–V trends alone are non-unique	[38,39,52,69]
Electrolyte loss/compositional change	Mass or volume loss; hermeticity/leakage testing; electrolyte spectroscopy/speciation; diffusion-related EIS	JSC and FF loss; diffusion limitation; eventual multi-parameter decay	Direct electrolyte measurements support Class A assignment; retention-only studies remain Class B	[24,80,81,96]
TCO/electrical-contact degradation	Four-point-probe or sheet-resistance mapping; contact resistance; microscopy; optical transmission	FF loss; increased series resistance; later JSC loss	Because series resistance is distributed across the device, TCO assignment without independent conductivity or morphological evidence remains inferential	[39,40]
Counter-electrode/metallic-grid degradation	Symmetric-cell EIS or CV; catalyst microscopy/composition; grid/contact resistance; corrosion inspection	FF loss; increased series or charge-transfer resistance; local current-collection loss	Component-resolved diagnostics are required to distinguish catalyst ageing from TCO or Ag-grid corrosion	[59,60]

10. Emerging Directions in Stability-Oriented DSSC Design

10.1. Solid-State and Hybrid DSSC Architectures

Eliminating volatile solvents is one of the most direct strategies for reducing electrolyte leakage and evaporation. Solid-state polymer electrolyte films demonstrate that relatively high PCE can be combined with substantial short-term stability when pore infiltration and interfacial contact are adequately controlled [91].

Solid-state p–n tandem DSSCs further demonstrate that sensitized photovoltaic architectures can be extended beyond conventional liquid-junction configurations while providing access to higher photovoltage [103]. Hybrid electrolyte strategies provide an in-

termediate approach by retaining liquid-like ionic transport while partially immobilising the electrolyte. PMMA- and PVDF-HFP-based gels, porous MOF hosts, and in situ-gelled copper electrolytes occupy different positions along the continuum between fully liquid and fully solid electrolyte systems [68,80,89,93]. The principal engineering challenge is to maintain effective pore filling and redox-species mobility while limiting macroscopic solvent movement and leakage. Recent polymer-gel, aqueous, COF-assisted, and module-oriented DSSC studies further support the development of hybrid electrolyte architectures that combine electrolyte retention with sufficient ionic transport [47,55,56,83,84].

A useful cross-technology perspective is provided by organic photovoltaics (OPVs), where solid-state absorber/transport stacks, interfacial layers, morphology control, and barrier engineering have been central to improving both charge extraction and durability [104]. Not all OPV concepts can be transferred directly to DSSCs because DSSCs rely on a mesoporous sensitized interface and redox regeneration; nevertheless, solvent-free or immobilised charge-transport media, conformal interlayers, and multilayer-barrier concepts provide relevant design principles for reducing leakage and limiting chemically aggressive contact between functional layers. For DSSCs, the key requirement is to preserve pore-scale interfacial contact and regeneration kinetics while gaining the packaging and materials-stability advantages associated with solid-state architectures.

10.2. Advanced Interface Engineering Approaches

Advanced interface engineering is increasingly moving from single-function blocking layers towards multifunctional interphases capable of simultaneously controlling interfacial chemistry, electrostatics, and charge transport. Compact TiO_2 layers can reduce FTO/electrolyte recombination; ultrathin polymeric interlayers can suppress back-electron transfer; hydrophobic additives can limit water interaction; and bio-derived modifiers can influence porosity and sensitizer adsorption [49,71,79,98]. These strategies may be combined provided that the resulting interfacial architecture does not introduce excessive transport resistance. Emerging passivation approaches based on MXenes, Ti^{3+}-modified TiO_2, carbon-assisted TiO_2 networks, and tailored molecular surface modifiers further illustrate the development of multifunctional interphases [70,74–77].

Molecular and device-level engineering are also becoming increasingly interconnected. Copper-compatible sensitizers and redox mediators can be designed as complementary components rather than independently optimised materials [61,62]. Deep eutectic solvent (DES)-based systems similarly demonstrate how sensitizer side-chain chemistry can be adapted to the local solvent environment [97]. Such co-design strategies provide a route to improving interfacial compatibility before additional protective layers are introduced. Future progress will therefore depend less on adding individual protective layers and more on co-designing chemically compatible interfaces that simultaneously control recombination, transport, and long-term chemical stability.

10.3. Multilayer Barrier and Encapsulation Concepts

Encapsulation materials typically involve trade-offs among moisture resistance, low-temperature processability, mechanical compliance, chemical compatibility, and optical stability. Multilayer barrier systems can therefore combine rigid low-permeability components with compliant polymeric layers and local chemical protection. In DSSCs, glass-frit sealing has demonstrated particularly effective long-term barrier performance, especially when electrolyte-filling ports are also hermetically sealed [51,99].

Future module-level encapsulation concepts should also address edge sealing, electrical feedthroughs, and current-collection pathways. Barrier structures should be evaluated with

respect to optical transmission and haze, thermal-expansion mismatch, mechanical integrity, and chemical compatibility with iodide-, cobalt-, or copper-based redox mediators.

At the module level, long-term durability will depend not only on the intrinsic stability of the active materials but also on the integrity of peripheral sealing and electrical interconnections.

10.4. Data-Driven and Predictive Stability Modelling

Data-driven stability modelling offers a complementary approach to experimental ageing because exhaustive long-term testing is impractical for every possible combination of sensitizers, electrolytes, interfaces, and device architectures. A 2025 machine-learning study based on 400 fabricated DSSCs demonstrated that long short-term memory (LSTM) models could reproduce degradation trajectories using interacting structural and electrolyte-related variables [78]. Such approaches can be used to explore multidimensional design spaces that would be difficult to investigate experimentally. Related data-driven and high-throughput studies are extending predictive analysis from device-level degradation behaviour to electrolyte formulation and optical or molecular descriptors associated with sensitizer/surface systems [48,65,94].

A particularly useful direction is the integration of data-driven prediction with physically interpretable degradation descriptors, including sensitizer-loading loss, recombination resistance, diffusion impedance, TCO sheet resistance, seal permeability, and cumulative environmental stress. Models trained only on PCE data may capture laboratory-specific correlations rather than broadly transferable degradation relationships. Consistent reporting practices and sufficiently large, shared ageing datasets could improve model transferability and facilitate the development of predictive tools capable of linking observed performance evolution with probable degradation mechanisms. A practical workflow connecting controlled ageing, diagnostic measurements, mechanistic interpretation, predictive modelling, and design feedback is summarised in Figure 4.

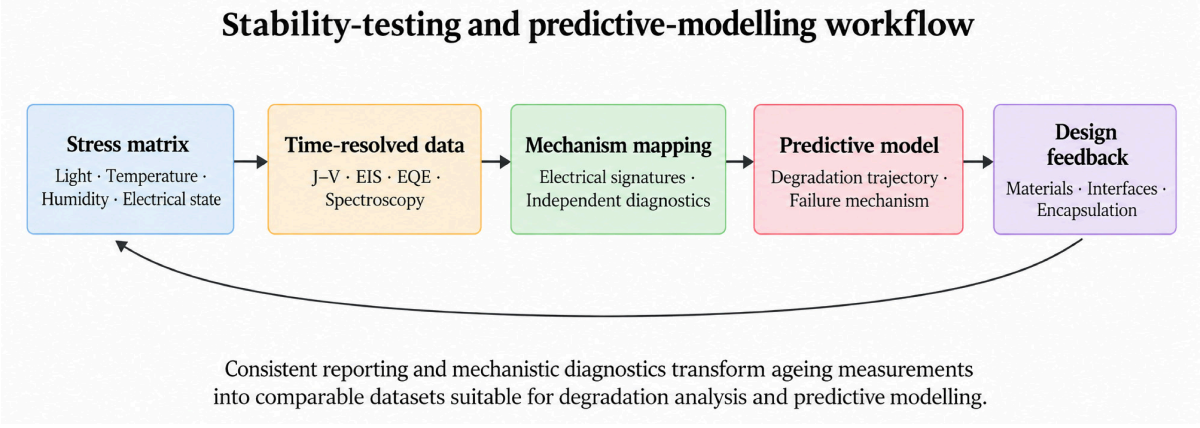


Figure 4. Stability-testing and predictive-modelling workflow linking controlled ageing conditions with time-resolved measurements, mechanistic interpretation, predictive analysis, and design feedback.

Predictive modelling should therefore complement rather than replace mechanistic experimentation, with the greatest value expected from models trained on standardised, time-resolved datasets that include both performance metrics and independent degradation descriptors. Predictive approaches should also include physically interpretable semi-analytical models rather than relying on machine learning alone. Chalkias, Loizos, and Papanicolaou combined one-diode analysis with a residual-property model to pre-

dict DSSC degradation under high- and low-temperature ageing, thermal-shock cycling, hydrothermal exposure, and reverse bias [105].

The model reproduced degradation trends across these accelerated conditions and illustrates how semi-analytical lifetime models can complement EIS and data-driven methods when datasets are too limited for robust machine learning. Their value is greatest when model parameters are linked to independently measured degradation variables rather than used only to extrapolate PCE-versus-time curves.

10.5. Scale-Up, Commercial Translation, and Application-Specific Reliability

Scale-up changes the reliability problem because resistive losses, electrolyte-distribution gradients, seal perimeter, current-collector corrosion, and spatial non-uniformity become increasingly important with device area. Large-area cells and modules therefore require stability criteria beyond those used for small laboratory devices, including spatial mapping of current collection, grid/contact resistance, seal integrity, and electrolyte distribution. In parallel-grid architectures, iodide-induced corrosion of metallic grids can become a primary lifetime limitation, whereas series-connected or monolithic modules introduce additional interconnect and sealing constraints [49,60]. Module-level stability should therefore be evaluated under the intended load and illumination regime rather than inferred from small-cell retention data.

Commercial activity further illustrates that DSSC deployment has become application-specific rather than centred on utility-scale one-sun competition. Ricoh commercialised solid-state indoor DSSC modules for IoT energy harvesting and reports operation over a temperature range from −30 to 60 °C; the company also states that electrolyte solidification eliminates the risk of liquid leakage due to ageing and improves product durability [106]. These statements are treated here as manufacturer-reported product information. Fujikura announced thin DSSC module panels intended for battery-free IoT devices [107]; because the cited manufacturer information does not provide a sufficiently detailed quantitative lifetime protocol, no numerical durability claim is assigned here. Peer-reviewed work co-authored by researchers from Taiwan DSC PV Ltd. (Taoyuan, Taiwan) evaluated cost-effective anthracene-based DSSCs under one-sun and dim-light conditions, with supporting module data reported under fluorescent illumination at 600 lux [108]. This study is therefore treated as performance/design evidence rather than as independent long-term lifetime validation. Solaronix supplies DSSC materials including Mosalyte non-volatile ionic-liquid electrolytes, which the manufacturer markets for high longevity and compatibility with high-temperature and diverse sealing processes [109]; these durability statements are likewise treated as manufacturer claims rather than independently validated lifetime evidence. Together, these examples document technological translation while reinforcing the need to distinguish commercial durability claims from peer-reviewed ageing results unless the test protocol, retention definition, and diagnostic evidence are disclosed.

The persistent one-sun efficiency gap relative to leading silicon and perovskite photovoltaics has both practical and intrinsic origins. DSSCs incur energetic losses associated with electron injection and dye regeneration, the redox-potential offset required for efficient regeneration, mass-transport limitations, and recombination at the large-area semiconductor/electrolyte interface; broad spectral harvesting is also constrained by sensitizer absorption and achievable surface coverage. Consequently, DSSCs are unlikely to compete with leading silicon or perovskite devices solely on peak outdoor PCE. Their stronger technological case lies in applications where spectral matching, transparency, colour tunability, bifacial response, low-light voltage, low-temperature processing, and autonomous energy harvesting dominate the system requirement [44,45]. This application-specific positioning also changes the relevant stability target: indoor IoT modules, agrivoltaic or

greenhouse glazing, and semi-transparent building elements require different stress profiles and lifetime metrics.

11. Conclusions

This review shows that DSSC durability is governed by coupled molecular, interfacial, electrolyte, current-collector, and packaging processes rather than by the instability of a single component. Its distinctive interface-centred and evidence-based framework links operational stressors to measured material changes, photovoltaic signatures, and mitigation strategies, while explicitly separating Class A mechanistically diagnosed ageing, Class B device-level retention, and Class C performance/design evidence. This distinction is essential because similar changes in J_{SC}, V_{OC}, FF, or PCE can originate from different failure locations.

The strongest evidence supports a systems approach to stability: robust sensitizer anchoring and regeneration, controlled TiO_2 surface chemistry, electrolyte confinement or solidification, chemically stable counter electrodes and current collectors, and effective encapsulation must operate together. Results obtained under one-sun light soaking, indoor illumination, thermal storage, outdoor exposure, and humidity–freeze testing should not be ranked by duration or PCE retention alone because these protocols probe different stress combinations. Large-area modules introduce additional failure modes through non-uniform electrolyte distribution, metallic-grid corrosion, interconnect resistance, and extended seal perimeters.

Five priorities emerge for future work: (1) report complete device architecture and stress history; (2) pair time-resolved photovoltaic tracking with at least one independent mechanistic diagnostic; (3) distinguish operational, storage, outdoor, and qualification-type tests and state whether measurements are in situ or post-recovery; (4) validate predictive and semi-analytical models against measured chemical or structural descriptors; and (5) evaluate scale-up and commercial architectures under application-specific loads. Progress should therefore be judged not only by the duration of PCE retention, but also by whether the suppressed degradation pathway is experimentally identified and remains controlled at module scale.

Author Contributions: Conceptualization, L.O. and S.S.-T.; methodology, L.O.; investigation, L.O.; literature analysis, L.O.; writing—original draft preparation, L.O.; writing—review and editing, L.O. and S.S.-T.; visualization, L.O.; supervision, S.S.-T. All authors have read and agreed to the published version of the manuscript.

Funding: This research received no external funding.

Data Availability Statement: No new data were created or analysed in this study. Data discussed in this review are available in the cited publications.

Acknowledgments: During the preparation of this manuscript, the authors used ChatGPT (OpenAI, GPT-5.6 Sol) for English-language editing and for assistance in preparing schematic graphical representations (Figures 1–4). The authors reviewed, edited, and validated all outputs and take full responsibility for the content of this publication.

Conflicts of Interest: The authors declare no conflicts of interest.

References

1. O'Regan, B.; Grätzel, M. A low-cost, high-efficiency solar cell based on dye-sensitized colloidal TiO_2 films. *Nature* **1991**, *353*, 737–740. [CrossRef]
2. Grätzel, M. Photoelectrochemical cells. *Nature* **2001**, *414*, 338–344. [CrossRef]
3. Siddiq, M.; Saxena, S.; Al Souwaileh, A.; Subbiah, J.; Anandan, S. Synthesis of $CuCo_2S_4$ nanosheets and its application in dye-sensitized solar cells. *Opt. Mater.* **2024**, *157*, 116367. [CrossRef]

4. Roy, P.; Vats, A.K.; Tang, L.; Kurokawa, Y.; Pandey, S.S. Controlling adsorption of two dyes on TiO_2 surface to improve the efficiency of see-through dye-sensitized solar cells. *Sol. Energy* **2024**, *269*, 112339. [CrossRef]
5. Yella, A.; Lee, H.-W.; Tsao, H.N.; Yi, C.; Chandiran, A.K.; Nazeeruddin, M.K.; Diau, E.W.-G.; Yeh, C.-Y.; Zakeeruddin, S.M.; Grätzel, M. Porphyrin-sensitized solar cells with cobalt(II/III)-based redox electrolyte exceed 12 percent efficiency. *Science* **2011**, *334*, 629–634. [CrossRef]
6. Mathew, S.; Yella, A.; Gao, P.; Humphry-Baker, R.; Curchod, B.F.E.; Ashari-Astani, N.; Tavernelli, I.; Rothlisberger, U.; Nazeeruddin, M.K.; Grätzel, M. Dye-sensitized solar cells with 13% efficiency achieved through the molecular engineering of porphyrin sensitizers. *Nat. Chem.* **2014**, *6*, 242–247. [CrossRef]
7. Kakiage, K.; Aoyama, Y.; Yano, T.; Oya, K.; Fujisawa, J.; Hanaya, M. Highly-efficient dye-sensitized solar cells with collaborative sensitization by silyl-anchor and carboxy-anchor dyes. *Chem. Commun.* **2015**, *51*, 15894–15897. [CrossRef]
8. Freitag, M.; Teuscher, J.; Saygili, Y.; Zhang, X.; Giordano, F.; Liska, P.; Hua, J.; Zakeeruddin, S.M.; Moser, J.-E.; Grätzel, M.; et al. Dye-sensitized solar cells for efficient power generation under ambient lighting. *Nat. Photonics* **2017**, *11*, 372–378. [CrossRef]
9. Rao, R.S.; Krishna, J.V.S.; Reddy, U.G.; Perepichka, I.F.; Shaya, J. Pyrazine-based sensitizers for dye-sensitized solar cells. *Mater. Chem. Front.* **2025**, *9*, 2120–2160. [CrossRef]
10. Rahmatian, M.; Sayyaadi, H.; Ameri, M. Indoor photovoltaics: A numerical model of dye-sensitized solar cells based on indoor illumination for the Internet of Things applications. *Energy Convers. Manag. X* **2024**, *22*, 100606. [CrossRef]
11. Szałas, G.; Zdyb, A. Three types of photovoltaic technologies under different artificial indoor light sources. *J. Ecol. Eng.* **2026**, *27*, 420–429. [CrossRef]
12. Vallejo, W.; Lerma, M.; Díaz-Uribe, C. Dye sensitized solar cells: Meta-analysis of effect sensitizer-type on photovoltaic efficiency. *Heliyon* **2025**, *11*, e41092. [CrossRef]
13. Marsya, M.A.; Lee, S.; Alvien, G.M.; Permanasari, I.N.P.; Choi, K.; Hong, J. Highly transparent dye-sensitized solar cells with UV-absorbing fluorene dyes and tetramethylthiourea electrolytes. *Sci. Rep.* **2025**, *15*, 43500. [CrossRef]
14. Barichello, J.; Mariani, P.; Vesce, L.; Spadaro, D.; Citro, I.; Matteocci, F.; Bartolotta, A.; Di Carlo, A.; Calogero, G. Bifacial dye-sensitized solar cells for indoor and outdoor renewable energy-based application. *J. Mater. Chem. C* **2024**, *12*, 2317–2349. [CrossRef]
15. Badawy, S.A.; Abdel-Latif, E.; Elmorsy, M.R. Tandem dye-sensitized solar cells achieve 12.89% efficiency using novel organic sensitizers. *Sci. Rep.* **2024**, *14*, 26072. [CrossRef]
16. Elmorsy, M.R.; Mohammed, S.M.; Mohamed, B.A.; Moustafa, A.H.; Badawy, S.A. High-efficiency tandem DSSCs based on tailored naphthalene sensitizers for indoor DSSC efficiency above 25%. *Sci. Rep.* **2025**, *15*, 44135. [CrossRef]
17. Kraidy, A.F.; Yapi, A.S.; Datte, J.K.; Voue, M.; El Marssi, M.; Ferri, A.; Gagou, Y. High-performance natural dye-sensitized solar cells employing a new semiconductor: $Gd_2Ru_2O_7$ pyrochlore oxide. *Condens. Matter* **2025**, *10*, 38. [CrossRef]
18. Rajkumar, S.; Venkatraman, M.R.; Arunkumar, A.; Jayaprakash, K. Anthocyanin and betalain pigments assisted green synthesis of TiO_2: A sustainable and cost-effective approach for dye-sensitized solar cells photoanodes. *Opt. Mater.* **2025**, *160*, 116710. [CrossRef]
19. AlSultan, H.A.; Shafie, S.; Hamidon, M.N.; Ismail, I.; Pandey, S.S.; Ahmad, F. Optimising bifacial dye-sensitized solar cells with graphene-enhanced TPT configuration photoanode for operational stability. *Sci. Rep.* **2025**, *15*, 38285. [CrossRef]
20. Ursu, D.; Vajda, M.; Ilieş, E.; Ricman, R.; Marinca, M.; Bularka, S.; Miclau, M.; Gontean, A. Towards the thermal stability of dye-sensitized solar cells for wavelength-selective greenhouses using the polymorphism of light-scattering layers. *Sustain. Energy Fuels* **2024**, *8*, 54–63. [CrossRef]
21. Sasitharan, K.; Freitag, M. From zombies to smart devices: The evolution of dye-sensitized solar cells for IoT applications. *ACS Appl. Energy Mater.* **2025**, *8*, 9891–9899. [CrossRef]
22. Yang, X.; Guo, Y.; Cheng, S. Ultrabroadband absorber based on titanium nitride concentric dual-ring array for high-efficiency solar energy harvesting. *Physica B* **2026**, *733*, 418581. [CrossRef]
23. Chen, Z.; Cheng, S.; Liu, M.; Li, B.; Tang, C.; Gao, F. Performance optimization of Cs2AgInBr6-based inorganic perovskite solar cells via hole transport layer engineering: A SCAPS-1D simulation study. *Mod. Phys. Lett. B* **2026**, *40*, 2650122. [CrossRef]
24. Farhana, N.K.; Pershaanaa, M.; Kamarulazam, F.; Saidi, N.M.; Bashir, S.; Ramesh, S.; Ramesh, K. A polysaccharide extracted from guar beans-based gel polymer electrolytes for efficient dye-sensitized solar cells. *J. Photochem. Photobiol. A Chem.* **2025**, *458*, 115963. [CrossRef]
25. Masud; Kim, H.K. Redox shuttle-based electrolytes for dye-sensitized solar cells: Comprehensive guidance, recent progress, and future perspective. *ACS Omega* **2023**, *8*, 6139–6163. [CrossRef]
26. Mittal, N.; Soni, R.K.; Sharma, V.; Prakhar, D.; Sharma, V.; Bharti; Singh, B.P.; Gupta, A.K.; Akitsu, T.; Sharma, R.K. Next-generation sensitizers for dye sensitizer solar cells: Molecular engineering, performance metrics, and photostability. *Sol. Compass* **2026**, *18*, 100161. [CrossRef]

27. Bužančić Milosavljević, M.; Perić Bakulić, M.; Sanader Maršić, Ž.; Mravak, A.; Bonačić-Koutecký, V. Enhancing efficiency of dye sensitized solar cells by coinage metal doping of cyanidin-silver trimer hybrids at TiO_2 support based on theoretical study. *Nanomaterials* **2024**, *14*, 1034. [CrossRef]
28. Gnida, P.; Schab-Balcerzak, E. Effect of structural and material modifications of dye-sensitized solar cells on photovoltaic performance. *Coatings* **2024**, *14*, 837. [CrossRef]
29. Brands, M.B.; Lugier, O.C.M.; Zhu, K.; Huijser, A.; Tanase, S.; Reek, J.N.H. Slow hole diffusion limits the efficiency of p-type dye-sensitized solar cells based on the P1 dye. *Energy Adv.* **2024**, *3*, 2035–2041. [CrossRef]
30. Consiglio, G.; Gorczyński, A.; Spoto, G.; Petralia, S.; Forte, G. Computational exploration of panchromatic dye-sensitized solar cells with broad visible to near-infrared absorption: A density functional theory study. *New J. Chem.* **2024**, *48*, 10026–10037. [CrossRef]
31. Nam, S.-H.; Ju, D.-W.; Boo, J.-H. Variations in power conversion efficiency on n-type dye-sensitized solar cells with synthesized TiO_2 nanoparticle: A thickness effect of active layer. *Catalysts* **2024**, *14*, 598. [CrossRef]
32. Kaushik, S.; Adesanya, M.A.; Hamann, T.W. Single component dye-sensitized solar cells enabled by copper chemistry: Introduction of the retro cell. *Energy Fuels* **2025**, *39*, 5604–5611. [CrossRef]
33. Trihutomo, P. Development of dye sensitized solar cell (DSSC) based on natural dye using dye solvent variation to increase efficiency. *EUREKA Phys. Eng.* **2026**, *2*, 36–44. [CrossRef]
34. Zhu, H.; Teale, S.; Lintangpradipto, M.N.; Mahesh, S.; Chen, B.; McGehee, M.D.; Sargent, E.H.; Bakr, O.M. Long-term operating stability in perovskite photovoltaics. *Nat. Rev. Mater.* **2023**, *8*, 569–586. [CrossRef]
35. Ren, Z.; Dolić, S.; Kojić, V.; Yuan, Z.; Troshin, P.; Gajović, A.; Popović, J.; Djurišić, A.B. Irreversible organic cations chemistry limits organic–inorganic halide perovskite stability under illumination or bias. *Nat. Energy* **2026**, *11*, 662–670. [CrossRef]
36. Sommeling, P.M.; Späth, M.; Smit, H.J.P.; Bakker, N.J.; Kroon, J.M. Long-term stability testing of dye-sensitized solar cells. *J. Photochem. Photobiol. A Chem.* **2004**, *164*, 137–144. [CrossRef]
37. Poskela, A.; Miettunen, K.; Tiihonen, A.; Lund, P.D. The state of external circuit affects the stability of dye-sensitized solar cells. *Electrochim. Acta* **2018**, *275*, 59–66. [CrossRef]
38. Zhang, C.; Huang, Y.; Chen, S.; Tian, H.; Mo, L.; Hu, L.; Huo, Z.; Kong, F.; Ma, Y.; Dai, S. Photoelectrochemical analysis of the dyed TiO2/electrolyte interface in long-term stability of dye-sensitized solar cells. *J. Phys. Chem. C* **2012**, *116*, 19807–19813. [CrossRef]
39. Bhatt, P.; Pandey, K.; Yadav, P.; Tripathi, B.; Kumar, M. Impedance spectroscopic investigation of the degraded dye-sensitized solar cell due to ageing. *Int. J. Photoenergy* **2016**, *2016*, 8523150. [CrossRef]
40. Sarker, S.; Seo, H.W.; Jin, Y.-K.; Aziz, M.A.; Kim, D.M. Transparent conducting oxides and their performance as substrates for counter electrodes of dye-sensitized solar cells. *Mater. Sci. Semicond. Process.* **2019**, *93*, 28–35. [CrossRef]
41. Asghar, M.I.; Miettunen, K.; Halme, J.; Vahermaa, P.; Toivola, M.; Aitola, K.; Lund, P. Review of stability for advanced dye solar cells. *Energy Environ. Sci.* **2010**, *3*, 418–426. [CrossRef]
42. Anitha, A.E.; Dotter, M. A Review on Liquid Electrolyte Stability Issues for Commercialization of Dye-Sensitized Solar Cells (DSSC). *Energies* **2023**, *16*, 5129. [CrossRef]
43. Iman, R.N.; Younas, M.; Harrabi, K.; Mekki, A. A comprehensive review on advancements and optimization strategies in dye-sensitized solar cells: Components, characterization, stability and efficiency enhancement. *Inorg. Chem. Commun.* **2024**, *169*, 112488. [CrossRef]
44. Zhou, H.; Aftabuzzaman, M.; Masud; Kang, S.H.; Kim, H.K. Key Materials and Fabrication Strategies for High-Performance Dye-Sensitized Solar Cells: Comprehensive Comparison and Perspective. *ACS Energy Lett.* **2025**, *10*, 881–895. [CrossRef]
45. Aftabuzzaman, M.; Zhou, H.; Masud; Akman, E.; Boruah, B.D.; Al-Ahmed, A.; Kim, H.K. Progress in highly efficient and stable dye-sensitized solar cells: State-of-the-art materials and device fabrication. *Coord. Chem. Rev.* **2026**, *563*, 218020. [CrossRef]
46. Al-Shamery, N.; Park, J.-H.; Kim, S.R.; Heppner, F.; Yoon, S.Y.; Bredow, T.; Kwon, T.-H.; Lee, P.S. From black pigment to green energy: Shedding light on melanin electrochemistry in dye-sensitized solar cells. *Mater. Adv.* **2025**, *6*, 3073–3083. [CrossRef]
47. Aftabuzzaman, M.; Masud; Kim, H.K. Stability and reliability of dye-sensitized solar-cell mini-module for photocharging Li-ion-battery-connected Internet of Things. *Sol. RRL* **2024**, *8*, 2300942. [CrossRef]
48. Plebankiewicz, I.; Bogdanowicz, K.A.; Kwaśnicki, P.; Przybył, W.; Skunik-Nuckowska, M.; Kulesza, P.J.; Iwan, A. Inorganic–organic modular silicon and dye-sensitized solar cells and predicted role of artificial intelligence towards efficient and stable solar chargers based on supercapacitors. *Sci. Rep.* **2024**, *14*, 6115. [CrossRef]
49. Kato, N.; Tanaka, H.; Takeda, Y.; Higuchi, K.; Nakajima, J. Demonstration of 12 years outdoor working of highly durable dye-sensitized solar cell modules employing hydrophobic surface passivation and suppression of biased distribution of iodine ions. *ACS Sustain. Chem. Eng.* **2023**, *11*, 4776–4785. [CrossRef]
50. Santos, F.; Martins, J.; Capitão, J.; Emami, S.; Ivanou, D.; Mendes, A. Stable cobalt-mediated monolithic dye-sensitized solar cells by full glass encapsulation. *ACS Appl. Energy Mater.* **2022**, *5*, 7220–7229. [CrossRef]
51. Capitão, J.; Martins, J.; Emami, S.; Ivanou, D.; Mendes, A. Fully glass frit encapsulated dye-sensitized solar cells: Challenges for hermetical sealing of electrolyte injection holes. *Sol. Energy* **2023**, *249*, 476–484. [CrossRef]

52. Ávila, M.; Cerdá, M.F. Thermodynamic and kinetics considerations in the competition between the dye regeneration and the recombination process in dye-sensitized solar cells. *Front. Coat. Dye. Interface Eng.* **2025**, *3*, 1527060. [CrossRef]
53. Xu, Z.; Xie, H.; Yu, T.; Zhu, C.; Zhang, J.; Zhu, H. Efficiency enhancement of indoor copper-based dye-sensitized solar cells by alkyl chain optimization in diketopyrrolopyrrole-based dyes with fence structure. *J. Photochem. Photobiol. A Chem.* **2025**, *473*, 116852. [CrossRef]
54. Nguyen, V.S.; Kannankutty, K.; Chen, Y.-H.; Wang, D.-C.; Yeh, C.-Y.; Wei, T.-C. Investigation on the coordination between methylpyridine additives and the $[Cu(dmp)_2]^{2+/+}$ redox couple and its improvement towards the stability of the dye-sensitized solar cells. *Sustain. Energy Fuels* **2024**, *8*, 2256–2264. [CrossRef]
55. Kandhasamy, M.; Shanmugam, G.; Duvaragan, B.K.; Kamaraj, S. Unleashing the potential of $Cu^{1+/2+}$ blended quasi-solid-state electrolytes for long-term stability of dye-sensitized solar cells. *Sol. Energy* **2024**, *277*, 112733. [CrossRef]
56. Sayah, D.; Ghaddar, T.H. Copper-based aqueous dye-sensitized solar cell: Seeking a sustainable and long-term stable device. *ACS Sustain. Chem. Eng.* **2024**, *12*, 6424–6432. [CrossRef]
57. Khazraei, S.; Mikladal, B.F.; Etula, J.; Varjos, I.; Hannu, J. Dry deposited single-walled carbon nanotubes co-assisted with copper redox mediator-based electrolytes for photo-stability of dye-sensitized solar cells. *Electrochim. Acta* **2024**, *488*, 144221. [CrossRef]
58. Sruthi, M.M.; Pradhan, S.C.; George, A.S.; Nitha, P.R.; Mishra, R.K.; John, J.; Soman, S. Exploring the synergy between copper electrolytes and molecularly engineered thiocyanate-free cyclometalated ruthenium sensitizers for dye-sensitized solar cells. *Photochem. Photobiol.* **2024**, *100*, 1127–1139. [CrossRef]
59. Kettle, J.; Aghaei, M.; Ahmad, S.; Fairbrother, A.; Irvine, S.; Jacobsson, J.J.; Kazim, S.; Kazukauskas, V.; Lamb, D.; Lobato, K.; et al. Review of technology-specific degradation in crystalline silicon, cadmium telluride, copper indium gallium selenide, dye sensitised, organic and perovskite solar cells in photovoltaic modules: Understanding how reliability improvements in mature technologies can enhance emerging technologies. *Prog. Photovolt. Res. Appl.* **2022**, *30*, 1365–1392. [CrossRef]
60. Son, M.-K.; Seo, H.; Kim, S.-K.; Hong, N.-Y.; Kim, B.-M.; Park, S.; Prabakar, K.; Kim, H.-J. Improved long-term durability of a parallel-type dye-sensitized solar cell module using a platinum metal grid fabricated by direct current magnetron sputtering with heat treatment. *J. Power Sources* **2013**, *222*, 333–339. [CrossRef]
61. Chen, Y.-H.; Chen, C.-C.; Nguyen, V.S.; Jiang, X.-T.; Chen, Y.-D.; Li, M.-Y.; Chen, S.-Y.; Wei, T.-C.; Yeh, C.-Y. A stable copper-modified bipyridine mediator for highly efficient dye-sensitized solar cells. *Cell Rep. Phys. Sci.* **2024**, *5*, 102159. [CrossRef]
62. Zhang, Y.; Higashino, T.; Namikawa, K.; Osterloh, W.R.; Imahori, H. Molecular engineering of porphyrin dyes and copper complexes for enhanced dye regeneration toward high-performance dye-sensitized solar cells using copper(I/II) redox shuttles. *Chem. Sci.* **2025**, *16*, 15004–15014. [CrossRef]
63. Chowdhury, A.; Wakchure, V.C.; Galleposo, E.C.; Bonifazi, D.; Costa, R.D. Cyano-borazine photosensitizers for dye-sensitized solar cells. *Adv. Energy Sustain. Res.* **2025**, *6*, 2400344. [CrossRef]
64. Hameed, I.H.; Ali, M.K.; Idrees, S.A. Co-sensitization effect of CNQDs and anthocyanin on TiO_2 for high-efficiency dye-sensitized solar cells: Experimental and theoretical insights. *ChemistrySelect* **2025**, *10*, e02197. [CrossRef]
65. Elsenety, M.M. High-throughput deep learning prediction of D-π-A dye absorption maxima on titania surfaces. *ChemistrySelect* **2025**, *10*, e01556. [CrossRef]
66. Abu-Melha, S. Enhanced light harvesting in dye-sensitized solar cells via triazole π-bridged organic dyes: Insights into co-sensitization and efficiency optimization. *J. Saudi Chem. Soc.* **2025**, *29*, 47. [CrossRef]
67. Yousef, S.H.; Abdel-Latif, E.; Badawy, S.A.; Elmorsy, M.R. Novel phenothiazine-based sensitizers for high-performance dye-sensitized solar cells: Enhanced photovoltaic properties through strategic co-sensitization with N719. *RSC Adv.* **2025**, *15*, 13896–13907. [CrossRef]
68. Afre, R.A.; Ryu, K.Y.; Shin, W.S.; Pugliese, D. Comparative study of quasi-solid-state dye-sensitized solar cells using Z907, N719, photoactive phenothiazine dyes and PVDF-HFP gel polymer electrolytes with different molecular weights. *Photonics* **2024**, *11*, 760. [CrossRef]
69. Adhikari, S.G.; Gascooke, J.R.; Kloo, L.; Andersson, G.G. Unveiling the aging effect at the interface of N719 dye-sensitized solar cells. *Adv. Mater. Interfaces* **2025**, *12*, 2400746. [CrossRef]
70. Camargo Matheus, A.P.; Gonçalves Larsson, L.F.; Taques Tractz, G.; Pinto Rodrigues, P.R. The TiO_2/electrolyte interface in DSSCs: An electrochemical study of the insertion of BTAH, BZM, and indole. *Opt. Mater.* **2025**, *159*, 116637. [CrossRef]
71. Masud; Noh, H.J.; Zhou, H.; Kang, S.H.; Aftabuzzaman, M.; Hasan, T.; Kim, H.K. Boosting the performance of dye-sensitized solar cells with an ultra-thin passivation layer of star-shaped block copolymer. *Surf. Interfaces* **2025**, *72*, 107124. [CrossRef]
72. Hsu, C.-Y.; Al-Salman, H.N.K.; Mahmoud, Z.H.; Ahmed, R.M.; Dawood, A.F. Improvement of the photoelectric dye sensitized solar cell performance using Fe/S–TiO_2 nanoparticles as photoanode electrode. *Sci. Rep.* **2024**, *14*, 4931. [CrossRef]
73. Lin, Y.-S.; Chen, W.-H. Dye-sensitized solar cells with modified TiO_2 scattering layer produced by hydrothermal method. *Materials* **2025**, *18*, 278. [CrossRef]
74. Srivastava, A.; Ito, Y.; Lee, H.; Ohshita, Y.; Ogura, A.; Dhonde, M.; Shirage, P.M. Multilayered 2D $Ti_3C_2T_X$-MXene: Best interfacial passivating agent for dye-sensitized solar cells with V_{OC} approaching 1 V. *ACS Appl. Electron. Mater.* **2025**, *7*, 1531–1549. [CrossRef]

75. Yıldız, Y.; Bilen, K.; Atılgan, A. Developing hybrid TiO_2–multiwalled carbon nanotubes photoanodes for dye-sensitized solar cells. *Energy Technol.* **2025**, *13*, 2401946. [CrossRef]
76. Nikhil, S.K.; Mathan Kumar, P.; Bhagavathiachari, M.; Nair, R.G. Enhancing the photoanode performance of dye-sensitized solar cells through integration of Cu doping and biphasic heterojunction in TiO_2. *Phys. Status Solidi A* **2025**, *222*, 2500219. [CrossRef]
77. Li, J.; Zhang, J.; Ling, Y.; Zhu, T.; Gan, K.; Nong, G. Introduction of Ti^{3+} within TiO_2 to improve photoanode electron transport performance in dye-sensitized solar cells (DSSCs). *Opt. Mater.* **2024**, *157*, 116226. [CrossRef]
78. Alali, A.S.; Ashraf, M.; Muhammad, A.; Abdellatif, S.O. Unveiling degradation patterns in dye-sensitized solar cells: A machine learning perspective. *Sci. Rep.* **2025**, *15*, 23820. [CrossRef]
79. Venkatesan, S.; Chang, Y.-C.; Teng, H.; Lee, Y.-L. Enhance the performance of dye-sensitized solar cells with effective compact layers and direct contact cell structure. *J. Power Sources* **2025**, *628*, 235889. [CrossRef]
80. Ibrayeva, A.; Imanbekova, Z.; Abibulla, U.; Tashenov, Y.; Baptayev, B.; Balanay, M.P. Enhancing the stability and efficiency of dye-sensitized solar cells with MIL-125 metal-organic framework as an electrolyte additive. *Sci. Rep.* **2025**, *15*, 5883. [CrossRef]
81. Mahalingam, S.; Manap, A.; Lau, K.S.; Floresyona, D.; Chia, C.H.; Afandi, N.; Chelvanathan, P.; Arith, F.; Nugroho, A. Improving dye-sensitized solar cell longevity: An aerogel encapsulation approach. *J. Taiwan Inst. Chem. Eng.* **2025**, *174*, 106207. [CrossRef]
82. Hatmanto, A.D.; Puspitaningrum, I.; Tefa, Y.N.C.; Santosa, S.J.; Kartini, I. Toward eco-friendly dye-sensitized solar cells: Developing chitosan-based electrolytes with conducting polymers and ionic liquids. *Int. J. Renew. Energy Dev.* **2025**, *14*, 727–739. [CrossRef]
83. Ibrayeva, A.; Suleimenova, D.; Imanbekova, Z.; Abibulla, U.; Baptayev, B.; Balanay, M.P. Engineering stable electrolytes with covalent organic frameworks to boost dye-sensitized solar cell efficiency. *Mater. Today Energy* **2025**, *54*, 102088. [CrossRef]
84. Varishetty, M.M.; Kenji, M.; Tarannum, N.; Damaraju, S.R.; Jonnalagadda, M. A novel poly(acrylonitrile)/poly(ethylene glycol)-based polymer gel electrolyte for high efficiency dye sensitized solar cells. *Energy Adv.* **2023**, *2*, 1702–1712. [CrossRef]
85. Rosa, E.S.; Septina, W.; Shobih; Megananda, P.C.; Hardian, A.; Nursam, N.M. Improved efficiency and stability of dye-sensitized solar cells by using iodide-based electrolyte with high viscosity solvent. *Mater. Lett.* **2024**, *358*, 135847. [CrossRef]
86. Jayadev, V.; Pradhan, S.C.; Nitha, P.R.; John, J.; Unni, K.N.N.; Soman, S. Investigating mass transport and recombination as a function of structural variation in dye-sensitized solar cells employing indole fused heterocyclic organic sensitizers and cobalt electrolytes. *J. Photochem. Photobiol.* **2024**, *19*, 100223. [CrossRef]
87. Meethal, S.M.; Pradhan, S.C.; Velore, J.; Varughese, S.; Pillai, R.S.; Sauvage, F.; Hagfeldt, A.; Soman, S. Asymmetric dual species copper(II/I) electrolyte dye-sensitized solar cells with 35.6% efficiency under indoor light. *J. Mater. Chem. A* **2024**, *12*, 1081–1093. [CrossRef]
88. Long, D.X.; Ghifari, M.A.; Yolthida, K.; Permanasari, I.N.P.; Hong, J. Strategic additive selection for advancing photovoltaic performance of liquid-electrolyte dye-sensitized solar cells. *Electrochim. Acta* **2025**, *511*, 145398. [CrossRef]
89. Sarwar, F.; Siddique, S.; Younas, M.; Gillani, S.E.H.; Akram, M.M.Z.; Saleem, B.; Mehmood, U. Molecular engineering of PMMA-based quasi-solid-state electrolytes for dye-sensitized solar cells: Tailoring ion conductivity and thermal stability through salt-ratio modulation. *Mater. Sci. Eng. B* **2025**, *314*, 118013. [CrossRef]
90. Goh, Z.L.; Farhana, N.K.; Kamarulazam, F.; Pershaanaa, M.; Bashir, S.; Ramesh, K.; Ramesh, S. Water as dual-function plasticizer and cosolvent in gel electrolytes for dye-sensitized solar cells. *Macromol. Rapid Commun.* **2025**, *46*, 2400481. [CrossRef]
91. Venkatesan, S.; Nguyen, H.T.M.; Teng, H.; Lee, Y.-L. Thin films of solid-state polymer electrolytes for dye-sensitized solar cells. *J. Power Sources* **2023**, *564*, 232896. [CrossRef]
92. Lee, Y.-H.; Venkatesan, S.; Wong, X.-W.; Lim, Z.Q.; Chang, L.-Y.; Lee, Y.-L.; Ho, K.-C. Ambient light harvesting with high-performance printable electrolyte in direct contact structured dye-sensitized solar cells. *Chem. Eng. J.* **2024**, *501*, 157506. [CrossRef]
93. Wong, X.-W.; Lee, Y.-H.; Venkatesan, S.; Ho, K.-C.; Teng, H.; Lee, Y.-L. Quasi-solid-state dye-sensitized solar cells with over 36% efficiency achieved by a direct-contact cell structure and in situ gelation of copper-based electrolytes. *ACS Sustain. Chem. Eng.* **2025**, *13*, 3432–3440. [CrossRef]
94. Liotier, J.; Riquelme, A.J.; Mwalukuku, V.; Huaulmé, Q.; Kervella, Y.; Demadrille, R.; Aumaître, C. Data-driven modelling for electrolyte optimisation in dye-sensitised solar cells and photochromic solar cells. *Mater. Horiz.* **2025**, *12*, 3803–3814. [CrossRef]
95. Amin, M.F.; Gnida, P.; Konieczkowska, J.; Szubka, M.; Schab-Balcerzak, E. Improvement of dye-sensitized solar cell performance via addition of azopyridine derivative in polymer gel electrolytes. *Materials* **2024**, *17*, 6107. [CrossRef]
96. Boldrini, C.L.; Quivelli, A.F.; Perna, F.M.; Biagini, P.; Capriati, V.; Abbotto, A.; Manfredi, N. Top-ranked efficiency under indoor light of DSSCs enabled by iodide-based DES-like solvent electrolyte. *Sustain. Energy Fuels* **2024**, *8*, 504–515. [CrossRef]
97. Salerno, G.; Boldrini, C.L.; Manfredi, N.; Capriati, V.; Bettucci, O.; Abbotto, A. Advancing dye-DES synergies in dye-sensitized solar cells for improved indoor efficiency and long-term stability under sustainable conditions. *Commun. Chem.* **2026**, *9*, 70. [CrossRef]

98. Rabelsa, G.; Shobih; Hidayat, J.; Milana, P.; Budiawan, W.; Almuqqodas, E.; Nursam, N.M.; Ibrahim, A.; Pranoto, L.M.; Firdaus, Y.; et al. The stability improvements of dye-sensitized solar cell with natural template for photoanode using lignin extracted from rice husk. *Heliyon* **2025**, *11*, e39913. [CrossRef]
99. Santos, F.; Martins, J.; Emami, S.; Ivanou, D.; Mendes, A. Ultralow temperature glass frit encapsulation for stable dye-sensitized solar cells. *ACS Appl. Energy Mater.* **2022**, *5*, 12598–12608. [CrossRef]
100. Martins, J.; Pereira, A.M.V.M.; Ivanou, D.; Mendes, A. Highly stable dye-sensitized solar cell using cobalt tris(bipyridyl) complexes via monolithic architecture. *Sol. RRL* **2025**, *9*, 2500310. [CrossRef]
101. Reese, M.O.; Gevorgyan, S.A.; Jørgensen, M.; Bundgaard, E.; Kurtz, S.R.; Ginley, D.S.; Olson, D.C.; Lloyd, M.T.; Morvillo, P.; Katz, E.A.; et al. Consensus stability testing protocols for organic photovoltaic materials and devices. *Sol. Energy Mater. Sol. Cells* **2011**, *95*, 1253–1267. [CrossRef]
102. Khenkin, M.V.; Katz, E.A.; Abate, A.; Bardizza, G.; Berry, J.J.; Brabec, C.; Brunetti, F.; Bulović, V.; Burlingame, Q.; Di Carlo, A.; et al. Consensus statement for stability assessment and reporting for perovskite photovoltaics based on ISOS procedures. *Nat. Energy* **2020**, *5*, 35–49. [CrossRef]
103. Wrede, S.; Cai, B.; Cheng, F.; Johansson, M.B.; Kubart, T.; Hägglund, C.; Tian, H. A solid-state p–n tandem dye-sensitized solar cell. *Sustain. Energy Fuels* **2024**, *8*, 1004–1011. [CrossRef]
104. Su, Y.-W.; Lan, S.-C.; Wei, K.-H. Organic photovoltaics. *Mater. Today* **2012**, *15*, 554–562. [CrossRef]
105. Chalkias, D.A.; Loizos, D.D.; Papanicolaou, G.C. Evaluation and prediction of dye-sensitized solar cells stability under different accelerated ageing conditions. *Sol. Energy* **2020**, *207*, 841–850. [CrossRef]
106. Ricoh Company, Ltd. Launch of New RICOH EH DSSC Modules with 20% Increase in Power Generation. 13 May 2021. Available online: https://www.ricoh.com/release/2021/0513_1 (accessed on 2 November 2026).
107. Fujikura Ltd. Launch of Thin Dye-Sensitized Solar Cell Module Panels—Expanded Product Lineup Enables Various IoT Devices to Eliminate the Need for Battery Replacement. 27 July 2020. Available online: https://www.fujikura.co.jp/en/news/pressrelease/20200727_iot.html (accessed on 2 November 2026).
108. Wang, C.-L.; Lin, P.-T.; Wang, Y.-F.; Chang, C.-W.; Lin, B.-Z.; Kuo, H.-H.; Hsu, C.-W.; Tu, S.-H.; Lin, C.-Y. Cost-Effective Anthryl Dyes for Dye-Sensitized Cells under One Sun and Dim Light. *J. Phys. Chem. C* **2015**, *119*, 24282–24289. [CrossRef]
109. Solaronix, S.A. Mosalyte, Non-Volatile Electrolytes. Available online: https://www.solaronix.com/materials/products/mosalyte/ (accessed on 2 November 2026).

Disclaimer/Publisher's Note: The statements, opinions and data contained in all publications are solely those of the individual author(s) and contributor(s) and not of MDPI and/or the editor(s). MDPI and/or the editor(s) disclaim responsibility for any injury to people or property resulting from any ideas, methods, instructions or products referred to in the content.